

Published in final edited form as:

*Biochemistry*. 2012 December 4; 51(48): 9736–9750. doi:10.1021/bi301024e.

## Specificity of Lipoprotein-Associated Phospholipase A<sub>2</sub> Towards Oxidized Phosphatidylserines: LC-ESI-MS Characterization of Products and Computer Modeling of Interactions

Vladimir A. Tyurin<sup>1,2</sup>, Naveena Yanamala<sup>1,3</sup>, Yulia Y. Tyurina<sup>1,2</sup>, Judith Klein-Seetharaman<sup>3</sup>, Colin H. Macphée<sup>3</sup>, and Valerian E. Kagan<sup>1,2</sup>

<sup>1</sup>Center for Free Radical and Antioxidant Health, University of Pittsburgh, Pittsburgh PA

<sup>2</sup>Department of Environmental & Occupational Health, University of Pittsburgh, Pittsburgh PA

<sup>3</sup>Department of Structural Biology, University of Pittsburgh, Pittsburgh PA

<sup>4</sup>GlaxoSmithKline, King of Prussia, PA, USA

### Abstract

Ca<sup>2+</sup> independent lipoprotein associated phospholipase A<sub>2</sub> (Lp-PLA<sub>2</sub>) is a member of the phospholipase A<sub>2</sub> superfamily with a distinguishing characteristic of high specificity for oxidatively modified *sn*-2 fatty acid residues in phospholipids which has been especially well characterized for peroxidized species of phosphatidylcholines (PC). The ability of Lp-PLA<sub>2</sub> to hydrolyze peroxidized species of phosphatidylserine (PS) – acting as a recognition signal for clearance of apoptotic cells by professional phagocytes - as well as the products of the reaction have not been investigated. We performed LC-MS-ESI-based structural characterization of oxygenated/hydrolyzed molecular species of PS - containing linoleic acid in either *sn*-2 position (C<sub>18:0</sub>/C<sub>18:2</sub>) or in both *sn*-1 and *sn*-2 positions (C<sub>18:2</sub>/C<sub>18:2</sub>) - formed in cytochrome *c*/H<sub>2</sub>O<sub>2</sub> driven enzymatic oxidation reaction. Cytochrome *c* has been chosen as a catalyst of peroxidation reactions due to its likely involvement in PS oxidation in apoptotic cells. We found that Lp-PLA<sub>2</sub> catalyzed the hydrolysis of both non-truncated and truncated (oxidatively fragmented) species of oxidized PS species albeit with different efficiencies and performed detailed characterization of the major reaction products – oxygenated derivatives of linoleic acid as well as non-oxygenated and oxygenated species of lyso-PS. Among linoleic acid products, derivatives oxygenated at the C<sub>9</sub> position, including 9-hydroxyoctadecadienoic acid (9-HODE) – a potent ligand of G protein-coupled receptor G2A - were the most abundant. Computer modeling of interactions of Lp-PLA<sub>2</sub> with different PS oxidized species indicated that they are able to bind in proximity (<5Å) to Ser273 and His351 of the catalytic triad. For 9-hydroxy- and 9-hydroperoxy- derivatives of oxidized PS, the *sn*-2 ester bond was positioned within the very close proximity (<3Å) from the Ser273 residue - a nucleophile directly attacking the *sn*-2 bond – thus favoring the hydrolysis reaction. We suggest that oxidatively modified free fatty acids and lyso-PS species generated by Lp-PLA<sub>2</sub> may represent important signals facilitating and regulating execution of apoptotic and phagocytosis programs essential for control of inflammation.

\*Corresponding authors: Valerian E. Kagan, PhD, DSc, Center for Free Radical and Antioxidant Health, Department of Environmental and Occupational Health, University of Pittsburgh, Bridgeside Point 100 Technology Drive, Suite 350, Pittsburgh, PA, USA. Tel: 412-624-9479, Fax: 412-624-9361, kagan@pitt.edu; Vladimir A. Tyurin, PhD, Center for Free Radical and Antioxidant Health Department of Environmental and Occupational Health, University of Pittsburgh Bridgeside Point, 100 Technology Drive, Suite 324 Pittsburgh, PA, USA, Tel: 412-383-5099, Fax: 412-624-9361, vtyurin@pitt.edu.

## Introduction

Diversity of phospholipids, including a large variety of their polyunsaturated species, is essential for normal physiology of mammalian cells.(1, 2) Most commonly, polyunsaturated acyl residues are localized in the *sn*-2 position whereas saturated and monounsaturated fatty acids are linked at the *sn*-1 position of the glycerol backbone. However saturated, mono- and polyunsaturated residues may be present in both *sn*-1 and *sn*-2 positions and the abundance of these species varies dependently on the type of tissue, cell or organelles as well as on nutritional and (patho)physiological conditions.(3, 4) For example, the level of polyunsaturated fatty acids esterified at the *sn*-1 position may significantly increase during phospholipid remodeling, transacylation, under low fat diet supplementation.(5, 6) The *sn*-position of polyunsaturated acyl residues in phospholipid glycerol backbone has a significant impact on the membrane function, cell signaling, and substrate specificity of various enzymes.(7)

The presence of multiple double bonds makes lipids susceptible to catalytic oxidative modifications with the addition of oxygen (lipid peroxidation) resulting in even greater variety and diversification of lipid species. The role of oxidized phospholipids as modulators of chronic inflammation, particularly in atherosclerosis, has been widely discussed.(2, 8, 9) Recent reports indicate that oxidized phospholipids may act as ligands for receptors that detect conserved pathogen-associated molecular patterns as an important part of innate immune defense. It is believed that the diversity of individual phospholipid oxidation products reflects their involvement in regulation of many aspects of the inflammatory processes.(2, 10-12)

Further diversification of oxidatively modified phospholipid species may be achieved via their hydrolysis by either phospholipase A<sub>1</sub> (PLA<sub>1</sub>) or phospholipase A<sub>2</sub> (PLA<sub>2</sub>) which cleave fatty acids from the *sn*-1 or *sn*-2 positions of glycerol backbone, respectively. The hydrolysis yields two types of products - free fatty acids (FFA) and lyso-phospholipids (lyso-PLs) that may also contain oxygenated functionalities. Polyunsaturated non oxidized and oxygenated FFA and their metabolites released from phospholipids are well recognized precursors of signaling molecules such as lipoxins, protectins and resolvins – significant players in the resolution of inflammation.(3, 13) Linoleic acid and its oxidized metabolites - abundant in LDL and atherosclerotic plaques – can act as regulators of macrophages differentiation and atherogenesis.(14, 15) Notably, in mammalian cells, polyunsaturated fatty acids especially linoleic acid, can be located in both *sn*-1 and *sn*-2 position of phosphatidylethanolamine and PS.(7) lyso-PLs (1-acyl-2lyso-PL or 2-acyl-1-lyso-PL) can also exhibit signaling capabilities, for example, through interaction with G protein-coupled receptors (GPR34) on target cells.(16, 17) Substantial concentrations of polyunsaturated lyso-phosphatidylcholine (lyso-PC, such as linoleoyl-lyso-PC and its hydroxy-derivatives) can accumulate in the heart and human plasma.(10, 11, 18)

In the 1970-80s, comparative assessments of the rates of PLA<sub>2</sub>-catalyzed hydrolysis of “peroxidized” *versus* intact phospholipids in membranes documented a higher PLA<sub>2</sub> activity towards membranes and liposomes enriched with oxidatively modified lipids.(19-21) More recently, a Ca<sup>2+</sup>-independent lipoprotein-associated phospholipase A<sub>2</sub> (Lp-PLA<sub>2</sub>) - also known as platelet-activating factor acetylhydrolase or type VIIA PLA<sub>2</sub> - actively secreted by monocyte-derived macrophages, has been shown to preferentially hydrolyze oxidatively modified phospholipids, particularly phosphatidylcholines (PC).(22-24) The enzyme is associated with circulating LDL in humans and with macrophages within atherosclerotic plaques and catalyzes the formation of lyso-PC and oxygenated FFA.

Although PS comprises a relatively minor fraction of membrane phospholipids, its regulatory functions are central to cell activity.(25) Clearance of apoptotic cells by professional phagocytes is largely dependent on the ability of the latter to recognize PS as well as its oxidation products on the surface of apoptotic cells.(26-33) The possibility of hydrolysis of externalized PS or its oxidation products and the role of this for the recognition of apoptotic cells by professional phagocytes and inflammatory response have not been considered. Interestingly, activation of a secretory PS-specific PLA<sub>1</sub> was detected at various sites of inflammation and has been implicated in the eicosanoid production.(34, 35) However, substrate specificity of PLAs towards different molecular species of peroxidized PS and their hydrolysis products are still insufficiently studied.

In this work, we performed LC-MS-based structural characterization of oxygenated/hydrolyzed molecular species of PS - containing linoleic acid in either *sn*-2 position C<sub>18:0</sub>/C<sub>18:2</sub> (SL-PS) or in both *sn*-1 and *sn*-2 positions C<sub>18:2</sub>/C<sub>18:2</sub> (LL-PS) - formed in cytochrome *c* (cyt *c*) driven enzymatic reaction in the presence of H<sub>2</sub>O<sub>2</sub>. Cyt *c* has been chosen as a catalyst of peroxidation reactions due to its likely involvement in PS oxidation in apoptotic cells.(29, 36, 37) Oxidation of SL-PS and LL-PS yielded oxygenated molecular species containing hydroxy-, hydroperoxy-, di-hydroxy-, hydroxy/hydroperoxy-, and di-hydroperoxy- groups at different carbon atoms (C<sub>8</sub>, C<sub>9</sub>, C<sub>12</sub>, C<sub>13</sub>, C<sub>14</sub>) of linoleic acid in *sn*-2 position. Further, LL-PS containing oxygenated linoleic acid in *sn*-1 position with one and two oxygens was detected. Small amounts of oxidatively fragmented (truncated) PS molecular species were also generated. Lp-PLA<sub>2</sub> catalyzed the hydrolysis of both non-truncated and truncated species of oxidized PS species albeit with different efficiencies. Computer modeling of interactions of Lp-PLA<sub>2</sub> with oxidized species of PS indicated that they bind in close proximity (<3Å) to a catalytic triad active site residue Ser<sub>273</sub>, favoring the hydrolysis of their *sn*-2 ester bond.

## MATERIALS AND METHODS

### Reagents

1,2-dioleoyl-*sn*-glycero-3-phosphocholine, DOPC, 1-stearoyl-2-linoleoyl-*sn*-glycero-3-phospho-L-serine, SL-PS, 1,2-linoleoyl-*sn*-glycero-3-phospho-L-serine, LL-PS, 1,2-diheptadecanoyl-*sn*-glycero-3-phospho-L-serine, PS (C<sub>17:0</sub>/C<sub>17:0</sub>), 1-stearoyl-2-hydroxy-*sn*-glycero-3-phospho-L-serine, (C<sub>18:0</sub>-lyso-PS), 1-tridecanoyl-2-hydroxy-*sn*-glycero-3-phospho-L-serine (C<sub>13:0</sub>-lyso-PS) were purchased from Avanti Polar Lipids Inc (Alabaster, AL) and were of the highest purity available. Recombinant human lipoprotein-associated phospholipase A<sub>2</sub> (Lp-PLA<sub>2</sub>) was obtained from GlaxoSmithKline Co (Collegeville, PA). Cytochrome *c* (cyt *c*), diethylenetriaminepentaacetic acid, PLA<sub>1</sub> from *Thermomyces lanuginosus*, DTPA, H<sub>2</sub>O<sub>2</sub> and all organic solvents (HPLC grade) were purchased from Sigma-Aldrich (St. Louis, MO). High purity lyso PS molecular species were obtained after their hydrolysis by porcine pancreas PLA<sub>2</sub> (Sigma-Aldrich, St. Louis, MO, USA) and subsequent separation by 2D-HPTLC. HPTLC silica G plates were purchased from Whatman (Schleicher & Schuell, England). Heptadecanoic acid (C<sub>17:0</sub>) was obtained from Matreya LLC (Pleasant Gap, PA). 9S-hydroperoxy-10E,12Z-octadecadienoic acid, 9S-hydroxy-10E,12Z-octadecadienoic acid, 13-oxo-9Z,11E-octadecadienoic acid, 13S-hydroxy-9Z,11E-octadecadienoic acid, 13S-hydroperoxy-9Z,11E-octadecadienoic acid, 9S-hydroxy-10E,12Z-octadecadienoic-9,10,12,13 d<sub>4</sub> acid, 9(10)epoxy-12Z-octadecenoic acid, 12(13)epoxy-9Z-octadecenoic acid were purchased from Cayman Chemical Co (Ann Arbor, Michigan, USA).

### Oxidation of phosphatidylserine

DOPC/PS (500  $\mu$ M, at a ratio of 1:1) liposomes were prepared by sonication in 50 mM HEPES buffer in the presence of 100  $\mu$ M DTPA pH 7.4. Liposomes, containing PS (250  $\mu$ M) were incubated with cyt *c* (5  $\mu$ M) and H<sub>2</sub>O<sub>2</sub> (100  $\mu$ M) during 30 min or 3 h at 37°C. At the end of incubation, lipids were extracted by Folch procedure (38) with minor modifications.

### Phospholipid hydrolysis by Lp-PLA<sub>2</sub>

Liposomes containing DOPC/PS were treated with Ca<sup>2+</sup>-independent secreted Lp-PLA<sub>2</sub> (0.26 - 2.6  $\mu$ g protein/sample) in 50 mM HEPES pH 8.2, containing 100  $\mu$ M DTPA for 30 min at 37°C. After incubation with Lp-PLA<sub>2</sub>, lipids were extracted and used for structural analysis by LC/ESI-MS.

### Phospholipid hydrolysis by PLA<sub>1</sub>

Liposomes containing DOPC/PS were treated with PLA<sub>1</sub> (2.4 - 24  $\mu$ g protein/sample) in 50 mM HEPES pH 7.4, containing 100  $\mu$ M DTPA for 30 min at 37°C. After incubation with PLA<sub>1</sub> lipids were extracted and used for structural analysis by LC-ESI-MS.

### Liquid chromatography/electro-spray ionization mass spectrometry (LC-ESI-MS) analysis

was performed on a Dionex HPLC system (utilizing the Chromeleon software) consisting of a Dionex UltiMate 3000 mobile phase pump, equipped with an UltiMate 3000 degassing unit; UltiMate 3000 autosampler (sampler chamber temperature was set at 4°C), 5  $\mu$ L sample loop. Dionex HPLC system was coupled to ion trap mass spectrometer (Finnigan™ LXQ™ with the Xcalibur operating system, Thermo Electron, San Jose, CA). The instrument was operated in the negative ion mode. For optimization of MS conditions and preparation of tune files, standards (2 pmol/ $\mu$ L) were injected by direct infusion through a syringe pump (flow rate 10  $\mu$ L/min) into the HPLC solvent flow (flow rate 200  $\mu$ L/min). The electrospray probe was operated at a voltage differential of 5.0 kV in the negative ion mode. Source temperature was maintained at 150°C. Spectra were acquired in negative ion mode using full range zoom (400-1600 *m/z* and 210 - 400 *m/z* for FFA) scans. Tandem mass spectrometry (MS/MS analysis) of individual PS species was used to determine the fatty acid composition. MS<sup>n</sup> analysis was carried out with relative collision energy ranging from 20-40% and with activation *q* value at 0.25 for collision-induced dissociation (CID) and *q* value at 0.7 for pulsed-Q dissociation (PQD) technique. MS/MS analysis was performed using isolation width of 1 *m/z*, 5 micro-scans with maximum injection time 1000 ms. For selected reaction monitoring (SRM) experiments the optimum collision energy was determined for each *m/z* parent daughter ion pair (30 kV).

### Normal phase column separation of phospholipids

Normal-phase LC conditions were as described by *Malavolta et al.*(39) with slight modifications. Phospholipids (5  $\mu$ L) were separated on a normal phase column (Luna 3  $\mu$ m Silica (2) 100A, 150×2 mm, (Phenomenex, Torrance, CA)) with flow rate 0.2 mL/min. The column was maintained at 30°C. The analysis was performed using gradient solvents (A and B). Solvent A was chloroform:methanol:ammonium hydroxide (28%), 80:19.5:0.5 (v/v). Solvent B was chloroform:methanol:water:ammonium hydroxide, 60:34:5:0.5 (v/v). The column was eluted during the first 3 min isocratic at 10% solvent B, 3 – 15 min with a linear gradient from 10% solvent B to 37% solvent B, 15 – 23 min linear gradient to 100% solvent B, and then 23 – 45 min isocratic at 100% solvent B, 47 - 57 min isocratic at 10% solvent B for equilibrium column. Reference standards of lyso PS for LC-ESI-MS analysis were obtained after hydrolysis of SL-PS and LL-PS by PLA<sub>2</sub> and following their separation by 2-D-HPTLC.

## Reverse phase column separation of fatty acids

FFA were separated on a reverse phase column (Luna 3  $\mu\text{m}$  C<sub>18</sub> (2) 100A, 150 $\times$ 2 mm, (Phenomenex)) at a flow rate of 0.2 mL/min. The column was maintained at 30°C. The analysis was performed using gradient solvents (A and B) containing 5 mM ammonium acetate. Solvent A was tetrahydrofuran/methanol/water/CH<sub>3</sub>COOH, 25:30:44.9:0.1 (v/v). Solvent B was methanol/water, 90:10 (v/v). The column was eluted during the first 3 min isocratically at 50% solvent B, from 3 to 23 min with a linear gradient from 50% solvent B to 98% solvent B, then 23 – 40 min isocratically using 98% solvent B, 40-42 min with a linear gradient from 98% solvent B to 50% solvent B, 42 - 48 min isocratically using 50% solvent B for equilibration of the column.

## Molecular docking studies

Three dimensional structures of SLPS, LLPS, SL-PSox and LL-PSox were generated using Marvin Sketch 5.3.6.(40) Hydroxy- and hydroperoxy-groups were placed at the *sn*-2 positions of SL-PS and LL-PS, yielding 9-hydroxy, 9-hydroperoxy, 9-hydroxy-14hydroxy, 9-hydroxy-12,13-epoxy, 9-hydroperoxy-14-hydroperoxy, 13-hydroxy, and 13-hydroperoxy species. Oxidatively-fragmented PS species containing either –oxo- or carboxy groups at the C<sub>9</sub> position (the end of truncation) were also created. These different species of oxidized PS were docked to the crystal structure of Lp-PLA<sub>2</sub> (PDBid: 3F9C using AutoDock Vina(41, 42) available at <http://vina.scripps.edu>. The lipid and Lp-PLA<sub>2</sub> 3D structures were converted from pdb into pdbqt format using MGL Tools.(43) The Lp-PLA<sub>2</sub> structure was treated as the receptor and was kept rigid during docking. In contrast, rotatable bonds in the lipid structures imparted flexibility on the ligands. A grid box was centered at the –14.59, –9.92, –32.08 coordinates with 70Å units in x, y and z directions to cover the active site of Lp-PLA<sub>2</sub>. Support for the chosen location of the grid box comes from a prediction of putative binding pockets by using Pocket-Finder software (<http://www.modelling.leeds.ac.uk/pocketfinder>). Using this independent approach, the active site was predicted to be the largest putative ligand binding site. Docking with Autodock Vina(42) resulted in 9 lowest energy conformations. Of these conformations, we concentrated on those binding poses where the *sn*-2 ester bond of the acyl chain was found in proximity to the active site. For docking purposes, proximity was defined as distance less than 5 Å to either residue Ser<sub>273</sub> or His<sub>315</sub> of the catalytic triad.

## RESULTS

### Structural characterization of oxidized SL-PS molecular species generated by cyt *c*/H<sub>2</sub>O<sub>2</sub>

We characterized cyt *c*/H<sub>2</sub>O<sub>2</sub> catalyzed oxidation of two PS species: SL-PS, and LL-PS, containing non-oxidizable stearic acid (C<sub>18:0</sub>) in the *sn*-1 position and oxidizable linoleic acid (C<sub>18:2</sub>) in the *sn*-2 position, or linoleic acid in both *sn*-1 and *sn*-2 positions, respectively. A complex mixture of oxidation products, containing 1, 2, 3 and 4 oxygens was documented by LC-MS profiles (Fig. 1A), MS<sup>1</sup> (Fig.1B) and MS<sup>2</sup> spectra (data not shown) of SL-PSox. Peroxidation of SL-PS (30 min at 37°C) resulted in the formation of several oxygenated products at *m/z* 802, 818, 834 and 850 corresponding to the following species: C<sub>18:0</sub>/C<sub>18:2</sub>+O, C<sub>18:0</sub>/C<sub>18:2</sub>+2O, C<sub>18:0</sub>/C<sub>18:2</sub>+3O and C<sub>18:0</sub>/C<sub>18:2</sub>+4O (Fig. 1C). Detailed MS<sup>2</sup> analysis demonstrated that the PS [M-H]<sup>-</sup> ions at *m/z* 802, 818, 834 and 850 contained mono-hydroxy, mono-hydroperoxy, di-hydroxy and di-hydroperoxy groups attached to either C<sub>9</sub> or C<sub>13</sub> carbons of linoleic acid (Table 1). Oxygenated molecular species of SL-PSox with *m/z* 800 containing oxidized isomers of 9-oxo- and 13-oxo-linoleic acid were also observed (data not shown). The molecular species with two oxygens (*m/z* 818) – corresponding to C<sub>18:0</sub>/C<sub>18:2</sub>+2O was dominant and its amount was estimated to be 9.4  $\pm$  1.0 mol% of SL-PS.

## Structural characterization of SL-PSox molecular species formed after hydrolysis of oxidized PS by Lp-PLA<sub>2</sub>

DOPC liposomes containing oxidized species of either SL-PS or LL-PS were treated with human recombinant Lp-PLA<sub>2</sub> and the hydrolysis products were analyzed by LC-ESI-MS. Typical LC-ESI-MS base-profiles of lyso-PS formed during hydrolysis of SL-PS with Lp-PLA<sub>2</sub> are presented in Fig. 2 Aab. Hydrolysis of SL-PS by Lp-PLA<sub>2</sub> yielded non-oxidized 1-stearoyl-2-lyso-PS (*m/z* 524) (Fig. 2Aa-c) and a mixture of free linoleic acid (*m/z* 279) along with a wide spectrum of its oxygenated metabolites (Fig. 3Aa). In line with previous reports, (19-21) significantly higher contents of hydrolysis products were found in the presence of peroxidized molecular PS species compared with non-oxidized PS (Fig. 2Ba-c). We found that Lp-PLA<sub>2</sub>-driven accumulation of lyso-PS was dependent on incubation time with enzyme (Fig. 2Ac). Further, the hydrolysis rate grew proportionally to the increased level of SL-PS oxidation (Fig. 2Ad) whereby oxidatively truncated species were preferable substrates for Lp-PLA<sub>2</sub> (Fig. 2Bc). Under our experimental conditions, no hydrolysis of non-oxidized DOPC was observed. This is consistent with the exclusive role of PS – compared to other classes of phospholipids as an activator of PLA<sub>2</sub>.(44) Expectedly, PLA<sub>1</sub>-induced hydrolysis of peroxidized SL-PS caused the release of stearic acid (*m/z* 283) and a mixture of lyso-PS with non oxygenated (*m/z* 520) and oxygenated linoleic acid (*m/z* 534, 536, 550, 552, 566, 568, 584) (data not shown).

Efficiency of Lp-PLA<sub>2</sub> hydrolysis of PSox species was proportional to the amount of oxygens present in the acyl chains (Fig 2Bc) and increased in the order: SL-PS (*m/z* 786) << SL-PSox (*m/z* 802) < SL-PSox (*m/z* 818) < SL-PSox (*m/z* 834) << SL-PSox (*m/z* 694). Quantitatively, the amounts of hydrolyzed SL-PS corresponded to the accumulated lyso-PS species. Because oxidatively fragmented PC species have been reported as substrates for Lp-PLA<sub>2</sub> (45) we were anxious to examine the effectiveness of the enzyme towards truncated species of PSox. To this end, we increased incubation time (up to 3h) for DOPC/SL-PS liposomes in the presence of cyt *c*/H<sub>2</sub>O<sub>2</sub>. This resulted in the significantly increased amounts of the major oxidized SL-PS species at *m/z* 818 (up to 40 Mol % of PS) and simultaneously to the appearance of relatively small amounts of oxidatively fragmented PS molecular species at *m/z* 678 and 694 corresponding to 1-stearoyl-2-(9-oxononanoyl)-sn-glycero-3-phosphoserine (ON-PS, 1 Mol % of PS) and 1-stearoyl-2-azelayl-sn-glycero-3-phosphoserine (A-PS, 3 Mol % of PS). In spite of their low abundance, these truncated PSox species were hydrolyzed with higher efficiency compared to other oxidized PS species (Fig. 2Bc). We further performed MS<sup>3</sup> analysis to determine which of the oxidatively modified PS acyls - oxygenated at the C<sub>9</sub> or C<sub>13</sub> carbon atoms - is a preferable substrate for the enzyme. MS<sup>n</sup> analysis of non-truncated SL-PSox, at *m/z* 818 (Fig. 2Cb) and *m/z* 802 (Fig. 2Cc) showed preferential cleavage of fatty acid residues containing hydroperoxy- and hydroxy-group at the C<sub>9</sub> position. This preference was also observed for the oxidatively fragmented species of PSox (Fig.2Ca). Accordingly, the remaining, non-hydrolyzed, SL-PSox (*m/z* 802) contained only 13-hydroxy-linoleic acid in the *sn*-2 position (Fig. 2Cd). The hydrolysis by Lp-PLA<sub>2</sub> – while overall effective towards SL-PSox – was still not 100% complete.

Characterization of the released oxidatively modified linoleic acid derivatives revealed the presence of molecular ions with *m/z* 295 that were identified as 9-hydroxy-, 13-hydroxy-linoleic acid and mixture of epoxy-derivatives of 9,10 epoxy- and 12,13 epoxy-linoleic acid (Fig. 3Ba, 3Bb). The amount of 9-hydroxy-isomers of linoleic acid hydrolyzed by Lp-LPA<sub>2</sub> was significantly higher (51.3 vs 18.1 pmol/nmol lysoPS, for SL-PS) compared with its 13-hydroxy-isomers (Fig, 3Bc). The same tendency was observed for 9,10 epoxy- and 12,13 epoxy- linoleic acid (*m/z* 295) (25.2 vs 5.3 pmol/nmol lysoPS, for SL-PS), respectively (Fig, 3Bc). Among the oxygenated FFA (with one oxygen), 9-oxo- and 13-oxo-linoleic acid (*m/z*

293) were found (data not shown). Cleaved oxygenated linoleic acid containing two oxygens was represented by 9-hydroperoxy-linoleic acid and a mixture of dihydroxy- (8,13-, 9,14-hydroxy- and 9-hydroxy-, 12,13-epoxy-) derivatives of linoleic acid, respectively (Fig. 3Ca, 3Cb, 3Cc).

### Structural characterization of oxidized LL-PS molecular species generated by cyt *c*/H<sub>2</sub>O<sub>2</sub>

Cyt *c*-driven oxidation of LL-PS yielded a large variety of oxidized species (Fig. 4AB, Table 2). LL-PS molecular species with oxidized linoleic acid residues containing 1, 2, 3 and 4 oxygens at *m/z* 798, 814, 830 and 846, respectively, were detected in the MS spectra (Fig. 4B). Quantitatively, significantly greater accumulation of oxidized products was found among modified molecular species of LL-PS compared to those formed from SL-PS (Fig. 4C). Expectedly, oxygenation of LL-PS occurred in both *sn*-1 and *sn*-2 positions whereby oxygenated species with oxygen(s) at C<sub>9</sub> and C<sub>13</sub> carbon atoms of linoleic acid were formed. Oxidation of linoleic acid in the *sn*-1 position was less pronounced compared with that localized in the *sn*-2 position. Interestingly, oxygenation in *sn*-1 position was observed only after the addition of two oxygens in *sn*-2 position in molecular species of LL-PSox (Table 2).

### Structural characterization of LL-PSox molecular species formed after hydrolysis of oxidized PS by Lp-PLA<sub>2</sub>

Typical LC-MS profiles of lyso-PS are presented in Fig 5Aa,b. Hydrolysis of oxidized LL-PS by Lp-PLA<sub>2</sub> revealed the presence of two types of lyso-PS products with either non-oxygenated (Fig. 5Ba) or oxygenated linoleic acid in *sn*-1 position (Fig. 5Bb). Non-oxidized 1-linoleoyl-2-lyso-PS with *m/z* 520 represented a dominant product, with smaller amounts of oxygenated lyso-PS species containing only one and two oxygens in the fatty acid moieties (*m/z* 534, 536 and 550, 552, respectively) (Fig. 5Bc). The total amount of accumulated lyso-PS was  $18.1 \pm 1.3$  Mol % of LL-PS, whereby the contents of non-oxidized-lyso-PS (1-linoleoyl-2-lyso-PS) and oxidized lyso-PS (1-oxidized linoleoyl-2-lyso-PS) were estimated as  $13.5 \pm 0.9$  and  $4.6 \pm 0.3$  Mol % of LL-PS, respectively (Fig. 5Bd). LL-PSox species were hydrolyzed with higher efficiency (Fig. 5Ca) yielding higher contents of hydrolysis products of PSox (Fig. 5Cb) compared with non-oxidized PS (Fig. 5Cc).

Similarly to SL-PSox, the preferable cleavage of oxygenated fatty acid residues containing hydroxy- and hydroperoxy groups in the C<sub>9</sub> position was observed for LL-PSox (data not shown). Interestingly, among products of LL-PSox hydrolysis, “heavily” oxygenated linoleic acid with 1-4 oxygens at C<sub>9</sub> or C<sub>13</sub> carbon atoms (*m/z* 293, 295, 309, 311, 325, 327, 343) were detected (Fig. 6A). MS<sup>2</sup> analysis of the liberated oxygenated linoleic acid revealed the presence of 9-hydroxy- and 13-hydroxy-, (Fig. 6Ba, Bb), 8,13-dihydroxy- (Fig. 6Ca, 6Cb) and 9,14-dihydroxy- (Fig. 6Ca, 6Cc) and 9-hydroperoxy-derivatives (data not shown). Quantitatively, the level of oxidized linoleic acid was significantly higher than the content of non-oxidized linoleic acid whereby hydroperoxy-molecular species were dominant. Overall,  $170.1 \pm 16.6$  pmol of oxidized and non-oxidized linoleic acid per nmol of LL-PS was released due to hydrolysis of oxidized LL-PS by Lp-PLA<sub>2</sub>. The contents of released oxidized and non-oxidized linoleic acid were  $154.4 \pm 13.1$  and  $15.7 \pm 2.7$  pmol/nmol LL-PS, respectively. These estimates are in good agreement with the data on Lp-PLA<sub>2</sub> catalyzed accumulation of lyso-PS (see above).

To further verify the localization of oxygenated linoleic acid residues generated by Lp-PLA<sub>2</sub> hydrolysis, we additionally utilized PLA<sub>1</sub>. In this case, the hydrolysis of oxidized LL-PS caused the release of non-oxidized plus oxidized linoleic acid (containing 1 and 2 oxygens only) (Fig. 7A) and oxidized species of lyso-PS containing oxygenated linoleic acid with 1-4 oxygens (*m/z* 536, 552, 568 and 584, respectively) (Fig. 7B). A lyso-PSox hydrolysis

product with  $m/z$  536 (containing 13-hydroxy-linoleic acid with  $m/z$  295) originated from two oxygenated molecular species of LL-PSox - one with  $m/z$  814 (containing trace amount of oxidized linoleic acid ( $m/z$  295) in *sn*-1 and *sn*-2 position) and the other one with  $m/z$  830 (containing oxidized linoleic acid ( $m/z$  295 and  $m/z$  311) in *sn*-1 and *sn*-2 positions, respectively) (Fig. 7C).

### Molecular modeling studies of LpPLA<sub>2</sub> interaction with lipids identified in this study

In an effort to better understand the specificity of Lp-PLA<sub>2</sub> catalysis, we performed docking studies of a total of 8 different species of PS and its oxidation products at different positions including C<sub>9</sub>, C<sub>13</sub> and C<sub>14</sub> as well as truncated species containing either oxo- or carboxy-groups at C<sub>9</sub> position. Specifically, 9-hydroxy, 9-hydroperoxy, 9,14-dihydroxy, 9-hydroxy-12,13-epoxy, 9,14-dihydroperoxy, 13-hydroxy, 13-hydroperoxy, truncated C<sub>9</sub>-oxo and C<sub>9</sub>-carboxy *sn*-2 species of both SL-PS and LL-PS were docked to the crystal structure of Lp-PLA<sub>2</sub> (PDBid : 3F9C, chain A)(41) to provide models for how different species interact with the protein that would help gain mechanistic insight into the molecular basis for the experimental data obtained. The active site of Lp-PLA<sub>2</sub> is characterized by a catalytic triad composed of residues Ser<sub>273</sub>, Asp<sub>296</sub> and His<sub>351</sub> (Fig. 8A), which accomplish hydrolysis of the *sn*-2 ester bond. Thus, we analyzed in detail those docking poses in which the *sn*-2 ester bond of the different oxidized species of SL-PS and LL-PS was located in proximity (within 5Å) to Ser<sub>273</sub> and His<sub>351</sub>. In particular, we looked for poses in which the side chain 'O' of Ser<sub>273</sub> was close to the *sn*-2 carbonyl 'O' and the *sn*-2 ester 'O' atom faced the closest His<sub>251</sub> 'N' atom (Fig. 8A, dashed lines). Table 3 lists the lowest binding energies, the number of poses satisfying this proximity criterion and the above-mentioned distances to Ser<sub>273</sub> and His<sub>351</sub> for the different oxidized species. The binding poses corresponding to -C<sub>9</sub>-oxo, -C<sub>9</sub>-carboxy, -9-hydroxy, -13-hydroperoxy, -9,14-dihydroxy of SL-PS and -9-hydroperoxy of both LL-PS and SL-PS species are shown in Fig. 8. In most cases, the phospholipid head groups of SL-PS and LL-PS bind close to a positively charged Lys<sub>370</sub> (Fig. 8). This residue was shown previously to play a role in binding of HDL(46) and LDL(47) to LpPLA<sub>2</sub>. The -OH of the serine head-group of PS in most cases points towards Lys<sub>370</sub> (Fig. 8B-D), although more rarely it points away from Lys<sub>370</sub> (Fig. 8E), albeit still in proximity. This proximity, particularly when the serine head-group is facing Lys<sub>370</sub>, leaves only one reasonable choice for the location of the *sn*-1 acyl chain, which is to be buried in a hydrophobic pocket (Fig. 8). In general, the position of the *sn*-1 chain in the hydrophobic pocket is independent of the lipid species analyzed. The *sn*-1 acyl chain binding site is similar to the proposed platelet activating factor (PAF) binding site.(41)

What is the mechanism by which oxidized lipids bind in proximity to the catalytic active site? Although the energies predicted for the different lipid species did not differ drastically, non-oxidized PS does bind less preferentially as compared to oxidized species of both SL-PS and LL-PS (Table 3). Furthermore, a relatively larger number of conformations were observed in proximity of the catalytic site (Table 3). A detailed analysis of the environment of the OH and OOH groups in the different high-ranking poses suggests that a number of interactions by these groups with the protein contribute favorably to binding (Table 4). In particular, OH and OOH groups were frequently observed to interact with aromatic residues in the binding pocket, in particular Phe<sub>322</sub> (in contact in poses for \*C9-O, \*C9-OOH, 9OOH, 9OH-14OH, 9OOH 14OOH) and Tyr<sub>324</sub> (for \*C9OOH, 9OH, 9OOH, 9OH-14OH, 9OOH-14OOH), but sometimes Phe<sub>110</sub> (for \*C9-OOH, 9OH-14OH), Tyr<sub>321</sub> (9OH-14OH) or Trp<sub>298</sub> (for \*C9-OOH, 9OH-14OH) were involved. Polar interactions also play a role in some conformations, such as with Arg<sub>218</sub> (for \*C9-O, \*C9-OOH, 9-OOH), Gln<sub>211</sub> (for \*C9-O), and Glu<sub>214</sub> (for \*C9-O, \*C9-OOH, 9OOH, 9OH-14OH). There are also intramolecular interactions within the lipids observed, such as with the PS-phosphate (\*C9-O, \*C9-OOH, 9OH, 9OOH) or the PS-amino group (9OH-14OH). Thus predicted stabilization of oxidized



lipids through molecular contacts is in line with the known specificity of Lp-PLA<sub>2</sub> towards oxidized phospholipids (45) and provides mechanistic insight in to the underlying reasons for the stabilization. Further, the *sn*-2 ester bond in both LL-PS and SL-PS was positioned in proximity to both Ser<sub>273</sub> and His<sub>351</sub> in the case of oxidatively fragmented species at the C<sub>9</sub> position as compared to C<sub>13</sub> position (Table 3). This suggests that one should expect the truncated *sn*-2 species to be preferred substrates, followed by C<sub>9</sub>-oxygenated non-truncated isomers, compared to C<sub>13</sub>-isomers - in line with the effectiveness of the hydrolysis of different oxidized PS species observed experimentally.

## DISCUSSION

As a member of the PLA<sub>2</sub> superfamily, Lp-PLA<sub>2</sub> has a distinguishing characteristic that it is highly specific for the type of the *sn*-2 residue to be hydrolyzed. In particular, phospholipid truncated oxidation products of the abundant *sn*-2 linoleoyl-containing phospholipids that harbor 9-carbon-long  $\omega$ -aldehyde or carboxylate functions, are efficiently hydrolyzed by the enzyme.(48) Because circulating Lp-PLA<sub>2</sub> is produced by inflammatory cells, bound to lipoproteins and accumulates in human atherosclerotic lesions – the role of the enzyme in metabolism of oxidized PC species was the major focus of many studies.(22, 45) Lp-PLA<sub>2</sub> effectively degrades oxidatively modified phospholipids present in oxidized LDL, particularly PCox, to yield two pro-inflammatory mediators - lyso-PC and oxidized non-esterified fatty acids – both of which may play a role in the development of atherosclerotic lesions and formation of a necrotic core, leading to more vulnerable plaques.(22, 23, 48-50) Recent work has documented essential role of oxidatively truncated PC and its Lp-PLA<sub>2</sub> hydrolysis products for TNF $\alpha$ -induced cell death.(51) The biological role of Lp-PLA<sub>2</sub> in metabolic conversions of other oxidatively modified phospholipids, particularly of anionic phospholipids, was largely neglected. Among the latter, PS and its oxidation products have been identified as signals essential for prompt and selective removal of “unwanted” or harmful cells, including apoptotic cells, acting as apoptotic cell-associated molecular patterns (ACAMPs).(52) Recognition of PS-based ACAMPs by specific macrophage receptors is an intrinsic part of “programmed clearance” of apoptotic cells at sites of inflammation that plays an important role in the resolution of the inflammatory process.(32)

Recently, we demonstrated that phospholipid peroxidation *in vivo* induced by a number of “oxidative stress” inducing factors - eg, gamma-irradiation, hyperoxia, traumatic brain injury – follows a specific non-random pattern in which two anionic phospholipids, a mitochondria-specific cardiolipin (CL), and extra-mitochondrial PS, represent the major oxidation substrates. In contrast, more abundant and highly polyunsaturated PC and phosphatidylethanolamine are not involved in the peroxidation process.(53, 54) We identified cyt *c* as a potent catalyst of these peroxidation reactions taking place in mitochondria early during the initiation of cell death program and in extra-mitochondrial compartments later during the execution of apoptosis.(28) Biologically, these peroxidation reactions were related to two signaling functions: i) participation of CL peroxidation products in mitochondrial membrane permeabilization(28) and ii) involvement of PS peroxidation products in the externalization process and recognition of PS and oxidatively modified PS species by putative receptors of professional phagocytes.(26) Possible hydrolysis of peroxidized species of either CL or PS by PLAs and likely roles of the hydrolysis products in regulation of apoptosis and phagocytosis have not been studied.

In the current work, we employed LC-MS to characterize the hydrolysis pathways of Lp-PLA<sub>2</sub> towards peroxidized species of PS. For the first time we demonstrated that oxidized PS can be used by Lp-PLA<sub>2</sub> as a substrate. Lp-PLA<sub>2</sub> is highly effective in catalyzing the hydrolysis of different non-truncated and truncated peroxidized species of SL-PSox and LL-PSox formed by cyt *c*/H<sub>2</sub>O<sub>2</sub> driven-catalysis. Expectedly, oxygenated species of linoleic

acid and non-oxidized stearyl-lyso-PS constituted the major products of hydrolysis when SL-PSox was used as a substrate. Notably, 9-isomers of oxygenated linoleic acid were dominating as hydrolysis products. Further, hydroxy-derivatives of linoleic acids, particularly the 9-hydroxy-form, participate in regulatory pathways through interaction with recently described receptor for long-chain fatty acids, G2A. The receptor mediates intracellular signaling events such as intracellular calcium mobilization and JNK activation as well as the secretion of cytokines (interleukin-6 and -8); it also blocks cell cycle progression at the G1 phase in response to ligands.(55)

We also established that oxidation of doubly polyunsaturated PS resulted in the formation of PS poly-oxygenated products with hydroperoxy- and hydroxy-groups located at both *sn*-1 and *sn*-2 positions. Lp-PLA<sub>2</sub> utilized 9-stereo-isomers of peroxidized LL-PS as a preferred substrate for the catalytic hydrolysis yielding 9-oxygenated derivatives of linoleic acid. Finally, Lp-PLA<sub>2</sub> is effective in catabolism of oxidatively fragmented PSox species - in line with previously demonstrated effectiveness of Lp-PLA<sub>2</sub> in hydrolyzing truncated oxidized PC species.(30, 45, 48) It is conceivable that both long-chain oxygenated derivatives of linoleic acid as well as its truncated oxidatively modified fragments will be released by Lp-PLA<sub>2</sub>. The yield of these respective products will be dependent on the relative abundance of different PS oxidation products which, in turn, are determined by specific peroxidation pathways. Considering that cyt *c* may be a major catalyst of PS oxidation in pro-apoptotic conditions, it is likely that oxygenated long-chain fatty acid residues may dominate as the products of PS peroxidation. Detailed analysis of these PS peroxidation/hydrolysis products may lead to the identification of meaningful biomarkers of non-random oxidative stress in phospholipids.

To obtain molecular insights into the underlying mechanisms for the experimentally found selectivity in hydrolysis of different lipid species, we investigated the structural basis for the interaction of Lp-PLA<sub>2</sub> with different oxidized and non-oxidized PS species. While a catalytic dyad with His and Asp residues has been identified in many PLA<sub>2</sub>s, a catalytically essential Ser<sub>273</sub> is present in two major cytosolic PLA<sub>2</sub>s - GIVA and GVIA (56) as well as in Lp-PLA<sub>2</sub>. In the latter case, the active site is composed of a catalytic triad involving Ser, His and Asp, whereby Ser<sub>273</sub> acts as a nucleophile that attacks the *sn*-2 ester bond of phospholipids. (57) Thus, the arrangement of the *sn*-2 ester bond in close proximity to Ser<sub>273</sub> might explain the specificity for differential hydrolysis observed experimentally for the different oxygenated molecular species. Especially, for the SL-PSox and LL-PSox species with a hydroxy- and hydroperoxy- group at the C<sub>9</sub> position (9-hydroxy- or 9-hydroperoxy-), which are hydrolyzed preferentially, the *sn*-2 ester bond of these species is predicted to bind very close (< 3Å) to Ser<sub>273</sub> compared to other species. Thus, the closer the oxygenated group is to the *sn*-2 ester bond of the species (i.e, oxygenation at C<sub>9</sub> is closer than C<sub>13</sub>), the more amenable that species is to hydrolysis by Lp-PLA<sub>2</sub>. While there are only subtle differences in the predicted energies between SL-PS and LL-PS, the conclusion that there is specificity of Lp-PLA<sub>2</sub> for C<sub>9</sub> versus C<sub>13</sub> oxidized lipids from the observed experimental results and the proximity to Ser<sub>273</sub> is further supported by the observation that multiple conformers are predicted to bind closer to the active site in the case of oxygenated species at C<sub>9</sub> position as compared to C<sub>13</sub>, regardless of SL-PSox versus LL-PSox. These results are also in agreement with previous studies which indicated that Lp-PLA<sub>2</sub> can cleave oxidized lipids in the *sn*-2 position up to 9 carbons long.(58)

In order to understand the mechanisms by which the *sn*-2 ester bond may be brought close to the active site, we investigated the different binding poses predicted by computer modeling. We find that the hydroxy- and hydroperoxy-groups in particular at the C<sub>9</sub> position bind in close proximity to aromatic residues that surround the binding pocket, especially Tyr<sub>324</sub> and Phe<sub>322</sub> (Fig. 8B,C, aromatics are shaded in pink). These residues may participate in the

stabilization of the interactions with these lipid species via OH donation by the oxidized lipids to pi systems of surrounding aromatic residues in Lp-PLA<sub>2</sub>. In the C13-OOH case, but also in some poses obtained for the truncated C9 species and in 9OOH, there is a stabilizing interaction with positive charges on Lp-PLA<sub>2</sub> (Fig. 8D). These additional stabilizing interactions afforded by the oxidation groups positions the sn 2 ester bond in oxidized species closer to the catalytic site, thus resulting in the experimentally observed preference observed in the hydrolysis of species with oxidation at C<sub>9</sub> position by Lp-PLA<sub>2</sub>. LC-MS experimental data indicates that truncated *sn*-2 species of oxidatively modified PS are better substrates for Lp-PLA<sub>2</sub> than respective long-chain oxygenated species of PS, consistent with the computer modeling results.

The information on possible involvement of oxidatively modified forms of PS and their metabolites in inflammation is starting to emerge. It has been shown that products of peroxidized PS hydrolysis - lyso-PS and oxygenated forms of linoleic acid - may act as signals by regulating anti- and pro-inflammatory responses.(14, 15) However, MS-based analysis of peroxidation/hydrolysis products formed from PS has not been performed. Our findings of oxygenated forms of lyso-PS whereby oxygenated fatty acid residues are located at either *sn*-1 or *sn*-2 positions suggest that these unusual PS species may be also involved in yet to be identified signaling pathways of apoptosis and phagocytosis possibly contributing to the development of inflammation. In fact, macrophage receptors – such as scavenger receptors and other putative receptors of PS and PSox – that mediate uptake of oxidatively modified lipoproteins - are also implicated in the recognition of apoptotic cells along with other known receptors – TIM-3, TIM-4, G2A.(59, 60) Interestingly, a recent study demonstrated a role for lyso-PS in enhancing the *in vitro* clearance of dying neutrophils via the G2A receptor.(31) It is noteworthy from the observations made in our studies that Lp-PLA<sub>2</sub> is capable of generating various ligands for the G2A receptor: HODEs, lyso-PS and lyso-PC. Moreover, PS and lyso-PLs are tightly bound to human CD1 molecules (a family of β<sub>2</sub>-microglobulin associated glycoproteins) at the cell surface and are involved in recognition by T lymphocytes.(59) Interestingly, oxidatively modified PC species have been reported to induce an unusual macrophage phenotype (Mox) that has been associated with the severity of atherosclerotic lesions and chronic inflammation.(61) Surprisingly, the influence of PSox species externalized on the surface of apoptotic cells - directly recognizable by macrophages(17, 31, 36) – as well as their hydrolysis products as determinants of macrophage phenotype in pro-inflammatory environments remains poorly understood.

Free radical peroxidation of phospholipids has been notoriously qualified as one of the major mechanisms of membrane damage occurring in a number of disease conditions. (62) The widely accepted concept of oxidative stress – induced by excessive formation of ROS and other radical intermediates – has leads to numerous clinical trials whose results and subsequent meta-analysis turned out to be less than satisfying.(8, 63-65) The reasons for these disappointments may be associated with poor understanding of enzymatic catalytic mechanisms involved in the production of “oxidative stress” as well as with under-appreciation of the specific signaling (rather than non-specific deleterious) roles of oxidatively modified lipids. While the pathways triggered by PLA<sub>2</sub>-driven release of eicosanoids, docosapentanooids and docosahexanooids and their subsequent oxygenation by cyclooxygenases and lipoxygenases have been well characterized (66, 67) the role and biology of peroxidized phospholipids as precursors of biologically active molecules is markedly less studied. Further investigations of the enzymatic metabolic pathways involved in peroxidation of phospholipids and subsequent hydrolysis of their oxidized species leading to the production of important lipid regulators are important. For example, the current work provides a reason to study the biological consequences of having apoptotic cells, together with their extracellular facing oxidized phospholipids, in close conjunction with secreted

Lp-PLA<sub>2</sub> derived from its primary cellular source, the professional phagocyte, the activated macrophage.

## Acknowledgments

Supported by NIH HL70755, ES020693, ES021068, U19 AIO68021, NS076511, and by NIOSH OH008282.

## ABBREVIATIONS

<b>A-PS</b>	stearoyl-azelayl-phosphatidylserine
<b>CL</b>	cardiolipin
<b>DTPA</b>	diethylenetriaminepentaacetic acid
<b>diHODE</b>	dihydroxy-octadecadienoic acid
<b>DOPC</b>	dioleoyl-phosphatidylcholine
<b>EpOME</b>	epoxy-octadecenoic acid
<b>FFA</b>	free fatty acids
<b>HpODE</b>	hydroperoxy-octadecadienoic acid
<b>HODE</b>	hydroxy-octadecadienoic acid
<b>Lp-PLA<sub>2</sub></b>	Lipoprotein-associated phospholipase A <sub>2</sub>
<b>LL-PS</b>	dilinoleoyl-phosphatidylserine
<b>Lyso-PL</b>	lyso-phospholipids
<b>PC</b>	phosphatidylcholine
<b>PS</b>	phosphatidylserine
<b>ON-PS</b>	stearoyl-oxononanoyl-phosphatidylserine
<b>SL-PS</b>	stearoyl-linoleoyl-phosphatidylserine

## REFERENCES

1. Dowhan W. Molecular basis for membrane phospholipid diversity: Why are there so many lipids? *Annu. Rev. Biochem.* 1997; 66:199–232. [PubMed: 9242906]
2. Furnkranz, A. a.; L., N. Regulation of Inflammatory Responses by Oxidized Phospholipids: Structure-Function Relationships. *Current Pharmaceutical Design.* 2004; 10:915–921. [PubMed: 15032694]
3. Bazan NG. Omega-3 fatty acids, pro-inflammatory signaling and neuroprotection. *Curr. Opin. Clin. Nutr. Metab. Care.* 2007; 10:136–141. [PubMed: 17285000]
4. Nakanishi H, Iida Y, Shimizu T, Taguchi R. Separation and quantification of sn-1 and sn-2 fatty acid positional isomers in phosphatidylcholine by RPLC-ESIMS/MS. *J Biochem.* 2010; 147:245–256. [PubMed: 19880374]
5. Dela I, Popovic M, Petrovic T, Delas F, Ivanovic D. Changes in the fatty acid composition of brain and liver phospholipids from rats fed fat-free diet. *Food Technol. Biotechnol.* 2008; 46:278–285.
6. Malhotra A, Edelman-Novemsky I, Xu Y, Plesken H, Ma J, Schlame M, Ren M. Role of calcium-independent phospholipase A2 in the pathogenesis of Barth syndrome. *Proc. Natl. Acad. Sci. U.S.A.* 2009; 106:2337–2341. [PubMed: 19164547]
7. Beermann C, Möbius M, Winterling N, Schmitt JJ, Boehm G. sn-Position determination of phospholipid-linked fatty acids derived from erythrocytes by liquid chromatography electrospray ionization ion-trap mass spectrometry. *Lipids.* 2005; 40:211–218. [PubMed: 15884770]

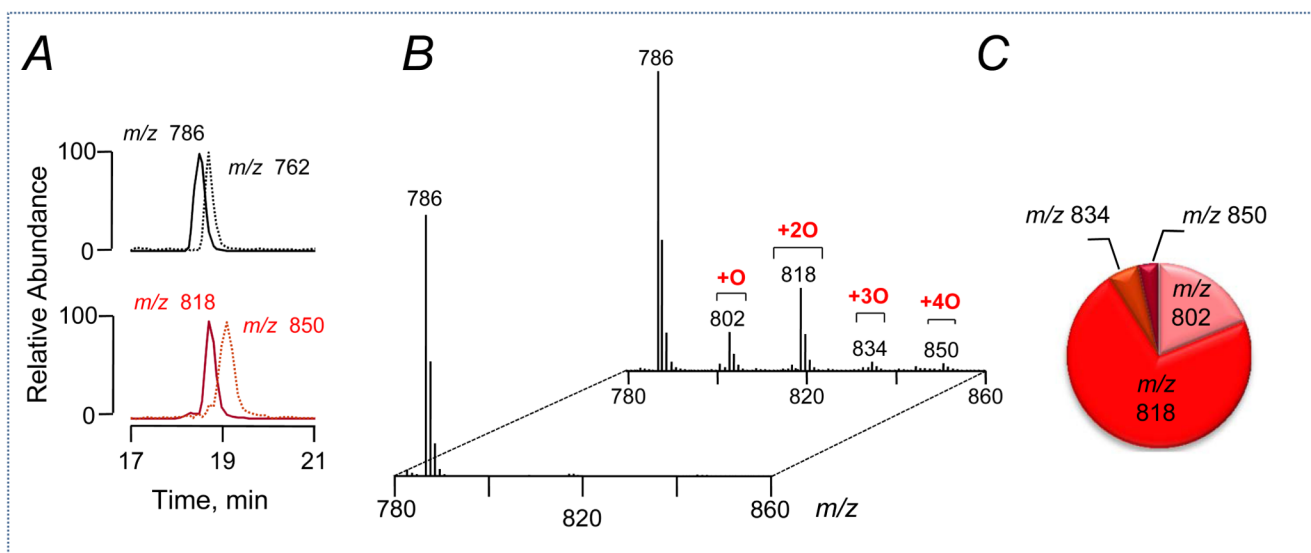
8. Leitinger N. Oxidized phospholipids as modulators of inflammation in atherosclerosis. *Curr. Opin. in Lipid.* 2003; 14:421–430.
9. Feldstein AE, Lopez R, Tamimi TA, Yerian L, Chung YM, Berk M, Zhang R, McIntyre TM, Hazen SL. Mass spectrometric profiling of oxidized lipid products in human nonalcoholic fatty liver disease and nonalcoholic steatohepatitis. *J. Lipid. Res.* 2010; 51:3046–3054. [PubMed: 20631297]
10. Adachi J, Asano M, Yoshioka N, Nushida H, Ueno Y. Analysis of phosphatidylcholine oxidation products in human plasma using quadrupole time-of-flight mass spectrometry. *Kobe J. Med. Sci.* 2006; 52:127–140. [PubMed: 17006053]
11. Barroso B, Bischoff R. LC-MS analysis of phospholipids and lysophospholipids in human bronchoalveolar lavage fluid. *J. Chromatogr. B Anal. Technol. Biomed. Life Sci.* 2005; 814:21–28.
12. Huang LS, Kim MR, Sok DE. Enzymatic reduction of polyunsaturated lysophosphatidylcholine hydroperoxides by glutathione peroxidase-1. *Eur. J. Lipid Sci. Technol.* 2009; 111:584–592.
13. Serhan CN, Chiang N, Van Dyke TE. Resolving inflammation: dual anti-inflammatory and pro-resolution lipid mediators. *Nat. Rev. Immunol.* 2008; 8:349–361. [PubMed: 18437155]
14. Jira W, Spitteller G, Carson W, Schramm A. Strong increase in hydroxy fatty acids derived from linoleic acid in human low density lipoproteins of atherosclerotic patients. *Chem. Phys. Lipids.* 1998; 91:1–11. [PubMed: 9488997]
15. Vangaveti V, Baune BT, Kennedy RL. Hydroxyoctadecadienoic acids: novel regulators of macrophage differentiation and atherogenesis. *Ther. Adv. Endocrinol. Metab.* 2010; 1:51–60. 51-60. [PubMed: 23148150]
16. Makidea K, Kitamura H, Sato Y, kutania M, Aoki J. Emerging lysophospholipid mediators, lysophosphatidylserine, lysophosphatidylthreonine, lysophosphatidylethanolamine and lysophosphatidylglycerol. *Prostagl. Other Lipid Mediators.* 2009; 89:135–139.
17. Frasch SC, Bratton DL. Emerging roles for lysophosphatidylserine in resolution of inflammation. *Prog. Lipid Res.* 2012; 51
18. Croset M, Brossard N, Polette A, Lagarde M. Characterization of plasma unsaturated lysophosphatidylcholines in human and rat. *Biochem. J.* 2000; 345:61–67. [PubMed: 10600639]
19. Kagan VE, Shvedova AA, Novikov KN. Participation of phospholipases in the “repair” of photoreceptor membranes subjected to peroxidation. *Biofizika.* 1978; 23:279–284. [PubMed: 306262]
20. Van Kuijk FJ, Sevanian A, Handelman GJ, Dratz EA. A new role for phospholipase A2: protection of membranes from lipid peroxidation damage. *Trends Biochem. Sci.* 1987; 12
21. Salgo MG, Corongiu FP, Sevanian A. Enhanced interfacial catalysis and hydrolytic specificity of phospholipase A2 toward peroxidized phosphatidylcholine vesicles. *Arch. Biochem. Biophys.* 1993; 304:123–132. [PubMed: 8323278]
22. Wilensky L, Shi Y, Mohler IER, Hamamdzc D, Burgert ME, Li J, Postle A, Fenning RS, Bollinger JG, Hoffman BE, Pelchovitz DJ, Yang J, Mirabile RC, Webb CL, LeFeng Zhang P, Gelb MH, Walker MC, Zalewski A, Macphee CH. Inhibition of lipoprotein-associated phospholipase A2 reduces complex coronary atherosclerotic plaque development. *Nat. Med.* 2008; 14:1059–1066. [PubMed: 18806801]
23. Wilensky RL, Macphee CH. Lipoprotein-associated phospholipase A(2) and atherosclerosis. *Curr. Opin. Lipidol.* 2009; 20:415–420. [PubMed: 19667981]
24. Kriska T, Marathe GK, Schmidt JC, McIntyre TM, Girotti AW. Phospholipase action of platelet-activating factor acetylhydrolase, but not paraoxonase-1, on long fatty acyl chain phospholipid hydroperoxides. *J. Biol. Chem.* 2007; 282:100–108. [PubMed: 17090529]
25. Fairm GD, Hermansson M, Somerharju P, Grinstein S. Phosphatidylserine is polarized and required for proper Cdc42 localization and for development of cell polarity. *Nature Cell Biol.* 2011; 13:1424–1430. [PubMed: 21964439]
26. Kagan VE, Gleiss B, Tyurina YY, Tyurin VA, Elenstrom-Magnusson C, Liu S-X, Serinkan FB, Arroyo A, Chandra J, Orrenius S, Fadeel B. A role for oxidative stress in apoptosis: Oxidation and externalization of phosphatidylserine is required for macrophage clearance of cells undergoing Fas-mediated apoptosis. *J. Immunol.* 2002; 169:487–499. [PubMed: 12077280]

27. Kagan VE, Borisenko GG, Tyurina YY, Tyurin VA, Jiang J, Potapovich AI, Kini V, Amoscato AA, Fujii Y. Oxidative lipidomics of apoptosis: Redox catalytic interactions of cytochrome c with cardiolipin and phosphatidylserine. *Free Radic. Biol. Med.* 2004; 37:1963–1985. [PubMed: 15544916]
28. Kagan VE, Tyurin VA, Jiang J, Tyurina YY, Ritov VB, Amoscato AA, Osipov AN, Belikova NA, Kapralov AA, Kini V, Vlasova II, Zhao Q, Zou M, Di P, Svistunenko DA, Kurnikov IV, Borisenko GG. Cytochrome c acts as a cardiolipin oxygenase required for release of proapoptotic factors. *Nature Chem. Biol.* 2005; 4:223–232. [PubMed: 16408039]
29. Tyurina YY, Kawai K, Tyurin VA, Liu SX, Kagan VE, Fabisiak JP. The plasma membrane is the site of selective phosphatidylserine oxidation during apoptosis: role of cytochrome c. *Antioxid. Redox Signal.* 2004; 6:209–225. [PubMed: 15025923]
30. Greenberg ME, Sun M, Zhang R, Febbraio M, Silverstein R, Hazen SL. Oxidized phosphatidylserine-CD36 interactions play an essential role in macrophage-dependent phagocytosis of apoptotic cells. *The Journal of experimental medicine.* 2006; 203:2613–2625. [PubMed: 17101731]
31. Frasch SC, Berry KZ, Fernandez-Boyanapalli R, Jin HS, Leslie C, Henson PM, Murphy RC, Bratton DL. NADPH oxidase-dependent generation of lysophosphatidylserine enhances clearance of activated and dying neutrophils via G2A. *The Journal of biological chemistry.* 2008; 283:33736–33749. [PubMed: 18824544]
32. Fadeel B, Xue D, Kagan V. Programmed cell clearance: molecular regulation of the elimination of apoptotic cell corpses and its role in the resolution of inflammation. *Biochemical and biophysical research communications.* 2010; 396:7–10. [PubMed: 20494102]
33. Ravichandran KS. Beginnings of a good apoptotic meal: the find-me and eat-me signaling pathways. *Immunity.* 2011; 35:445–455. [PubMed: 22035837]
34. Hosono H, Aoki J, Nagai Y, Bandoh K, Ishida M, Taguchi R, Arai H, Inoue K. Phosphatidylserine-specific phospholipase A1 stimulates histamine release from rat peritoneal mast cells through production of 2-acyl-1-lysophosphatidylserine. *The Journal of biological chemistry.* 2001; 276:29664–29670. [PubMed: 11395520]
35. Aoki J, Nagai Y, Hosono H, Inoue K, Arai H. Structure and function of phosphatidylserine-specific phospholipase A1. *Biochimica et biophysica acta.* 2002; 1582:26–32. [PubMed: 12069807]
36. Tyurina YY, Serinkan FB, Tyurin VA, Kini V, Yalowich JC, Schroit AJ, Fadeel B, Kagan VE. Lipid antioxidant, etoposide, inhibits phosphatidylserine externalization and macrophage clearance of apoptotic cells by preventing phosphatidylserine oxidation. *The Journal of biological chemistry.* 2004; 279:6056–6064. [PubMed: 14630936]
37. Tyurin VA, Tyurina YY, Feng W, Mnuskin A, Jiang J, Tang M, Zhang X, Zhao Q, Kochanek PM, Clark RS, Bayir H, Kagan VE. Mass-spectrometric characterization of phospholipids and their primary peroxidation products in rat cortical neurons during staurosporine-induced apoptosis. *Journal of neurochemistry.* 2008; 107:1614–1633. [PubMed: 19014376]
38. Folch J, Lees M, Sloane Stanley GH. A simple method for the isolation and purification of total lipides from animal tissues. *The Journal of biological chemistry.* 1957; 226:497–509. [PubMed: 13428781]
39. Malavolta M, Bocci F, Boselli E, Frega NG. Normal phase liquid chromatography-electrospray ionization tandem mass spectrometry analysis of phospholipid molecular species in blood mononuclear cells: application to cystic fibrosis. *Journal of chromatography. B, Analytical technologies in the biomedical and life sciences.* 2004; 810:173–186.
40. Marvin Sketch was used for drawing, displaying the chemical structures and generating the 3D structures corresponding to the lowest energy conformer, Marvin 5.3.6. ChemAxon; 2010. <http://www.chemaxon.com>
41. Samanta U, Kirby SD, Srinivasan P, Cerasoli DM, Bahnson BJ. Crystal structures of human group-VIIA phospholipase A2 inhibited by organophosphorus nerve agents exhibit non-aged complexes. *Biochemical pharmacology.* 2009; 78:420–429. [PubMed: 19394314]
42. Trott O, Olson AJ. AutoDock Vina: improving the speed and accuracy of docking with a new scoring function, efficient optimization, and multithreading. *Journal of computational chemistry.* 2010; 31:455–461. [PubMed: 19499576]

43. Sanner MF, Duncan BS, Carrillo CJ, Olson AJ. Integrating computation and visualization for biomolecular analysis: an example using python and AVS. Pacific Symposium on Biocomputing. Pacific Symposium on Biocomputing. 1999;401–412. [PubMed: 10380214]
44. Lee T, Malone B, Longobardi L, Balestrieri ML. Differential regulation of three catalytic activities of platelet-activating factor (PAF)-dependent transacetylase. Archives of biochemistry and biophysics. 2001; 387:41–46. [PubMed: 11368182]
45. Davis B, Koster G, Douet LJ, Scigelova M, Woffendin G, Ward JM, Smith A, Humphries J, Burnand KG, Macphee CH, Postle AD. Electrospray ionization mass spectrometry identifies substrates and products of lipoprotein-associated phospholipase A2 in oxidized human low density lipoprotein. The Journal of biological chemistry. 2008; 283:6428–6437. [PubMed: 18165686]
46. Gardner AA, Reichert EC, Topham MK, Stafforini DM. Identification of a domain that mediates association of platelet activating factor acetylhydrolase with high density lipoprotein. The Journal of biological chemistry. 2008; 283:17099–17106. [PubMed: 18434304]
47. Stafforini DM, Tjoelker LW, McCormick SP, Vaitkus D, McIntyre TM, Gray PW, Young SG, Prescott SM. Molecular basis of the interaction between plasma platelet-activating factor acetylhydrolase and low density lipoprotein. The Journal of biological chemistry. 1999; 274:7018–7024. [PubMed: 10066756]
48. McIntyre TM, Prescott SM, Stafforini DM. The emerging roles of PAF acetylhydrolase. Journal of lipid research. 2009; 50(Suppl):S255–259. [PubMed: 18838739]
49. Chauffe RJ, Wilensky RL, Mohler ER 3rd. Recent developments with lipoprotein-associated phospholipase A2 inhibitors. Current atherosclerosis reports. 2010; 12:43–47. [PubMed: 20425270]
50. Magrioti V, Kokotos G. Phospholipase A2 inhibitors as potential therapeutic agents for the treatment of inflammatory diseases. Expert opinion on therapeutic patents. 2010; 20:1–18. [PubMed: 20021282]
51. Latchoumycandane C, Marathe GK, Zhang R, McIntyre TM. Oxidatively truncated phospholipids are required agents of tumor necrosis factor alpha (TNFalpha)-induced apoptosis. The Journal of biological chemistry. 2012; 287:17693–17705. [PubMed: 22433871]
52. Nakanishi Y, Henson PM, Shiratsuchi A. Pattern recognition in phagocytic clearance of altered self. Advances in experimental medicine and biology. 2009; 653:129–138. [PubMed: 19799116]
53. Tyurina YY, Tyurin VA, Epperly MW, Greenberger JS, Kagan VE. Oxidative lipidomics of gamma-irradiation-induced intestinal injury. Free radical biology & medicine. 2008; 44:299–314. [PubMed: 18215738]
54. Tyurina YY, Tyurin VA, Kaynar AM, Kapralova VI, Wasserloos K, Li J, Mosher M, Wright L, Wipf P, Watkins S, Pitt BR, Kagan VE. Oxidative lipidomics of hyperoxic acute lung injury: mass spectrometric characterization of cardiolipin and phosphatidylserine peroxidation. American journal of physiology. Lung cellular and molecular physiology. 2010; 299:L73–85. [PubMed: 20418384]
55. Obinata H, Izumi T. G2A as a receptor for oxidized free fatty acids. Prostag Oth Lipid M. 2009; 89:66–72.
56. Kokotos G, Hsu YH, Burke JE, Baskakis C, Kokotos CG, Magrioti V, Dennis EA. Potent and selective fluoroketone inhibitors of group VIA calcium-independent phospholipase A2. Journal of medicinal chemistry. 2010; 53:3602–3610. [PubMed: 20369880]
57. Dennis EA, Cao J, Hsu YH, Magrioti V, Kokotos G. Phospholipase A2 enzymes: physical structure, biological function, disease implication, chemical inhibition, and therapeutic intervention. Chemical reviews. 2011; 111:6130–6185. [PubMed: 21910409]
58. Min JH, Jain MK, Wilder C, Paul L, Apitz Castro R, Aspleaf DC, Gelb MH. Membrane-bound plasma platelet activating factor acetylhydrolase acts on substrate in the aqueous phase. Biochemistry. 1999; 38:12935–12942. [PubMed: 10504265]
59. Cox D, Fox L, Tian R, Bardet W, Skaley M, Mojsilovic D, Gumperz J, Hildebrand W. Determination of cellular lipids bound to human CD1d molecules. PloS one. 2009; 4:e5325. [PubMed: 19415116]

60. Freeman GJ, Casasnovas JM, Umetsu DT, DeKruyff RH. TIM genes: a family of cell surface phosphatidylserine receptors that regulate innate and adaptive immunity. *Immunological reviews*. 2010; 235:172–189. [PubMed: 20536563]
61. Kadl A, Bochkov VN, Huber J, Leitinger N. Apoptotic cells as sources for biologically active oxidized phospholipids. *Antioxidants & redox signaling*. 2004; 6:311–320. [PubMed: 15025932]
62. Niki E. Lipid peroxidation: physiological levels and dual biological effects. *Free radical biology & medicine*. 2009; 47:469–484. [PubMed: 19500666]
63. Griendling KK, FitzGerald GA. Oxidative stress and cardiovascular injury: Part II: animal and human studies. *Circulation*. 2003; 108:2034–2040. [PubMed: 14581381]
64. Poulsen HE, Andersen JT, Keiding N, Schramm TK, Sorensen R, Gisslasson G, Fosbol EL, Torp-Pedersen C. Why epidemiological and clinical intervention studies often give different or diverging results? *IUBMB life*. 2009; 61:391–393. [PubMed: 18975376]
65. Azzi A. Oxidative stress: A dead end or a laboratory hypothesis? *Biochemical and biophysical research communications*. 2007; 362:230–232. [PubMed: 17686462]
66. Bazan NG. Cellular and molecular events mediated by docosahexaenoic acid-derived neuroprotectin D1 signaling in photoreceptor cell survival and brain protection. *Prostaglandins, leukotrienes, and essential fatty acids*. 2009; 81:205–211.
67. Gleissman H, Yang R, Martinod K, Lindskog M, Serhan CN, Johnsen JI, Kogner P. Docosahexaenoic acid metabolome in neural tumors: identification of cytotoxic intermediates. *FASEB journal : official publication of the Federation of American Societies for Experimental Biology*. 2010; 24:906–915. [PubMed: 19890019]
68. DeLano, WL. *The PyMOL User's Manual*. DeLano Scientific; Palo Alto, CA: 2002.





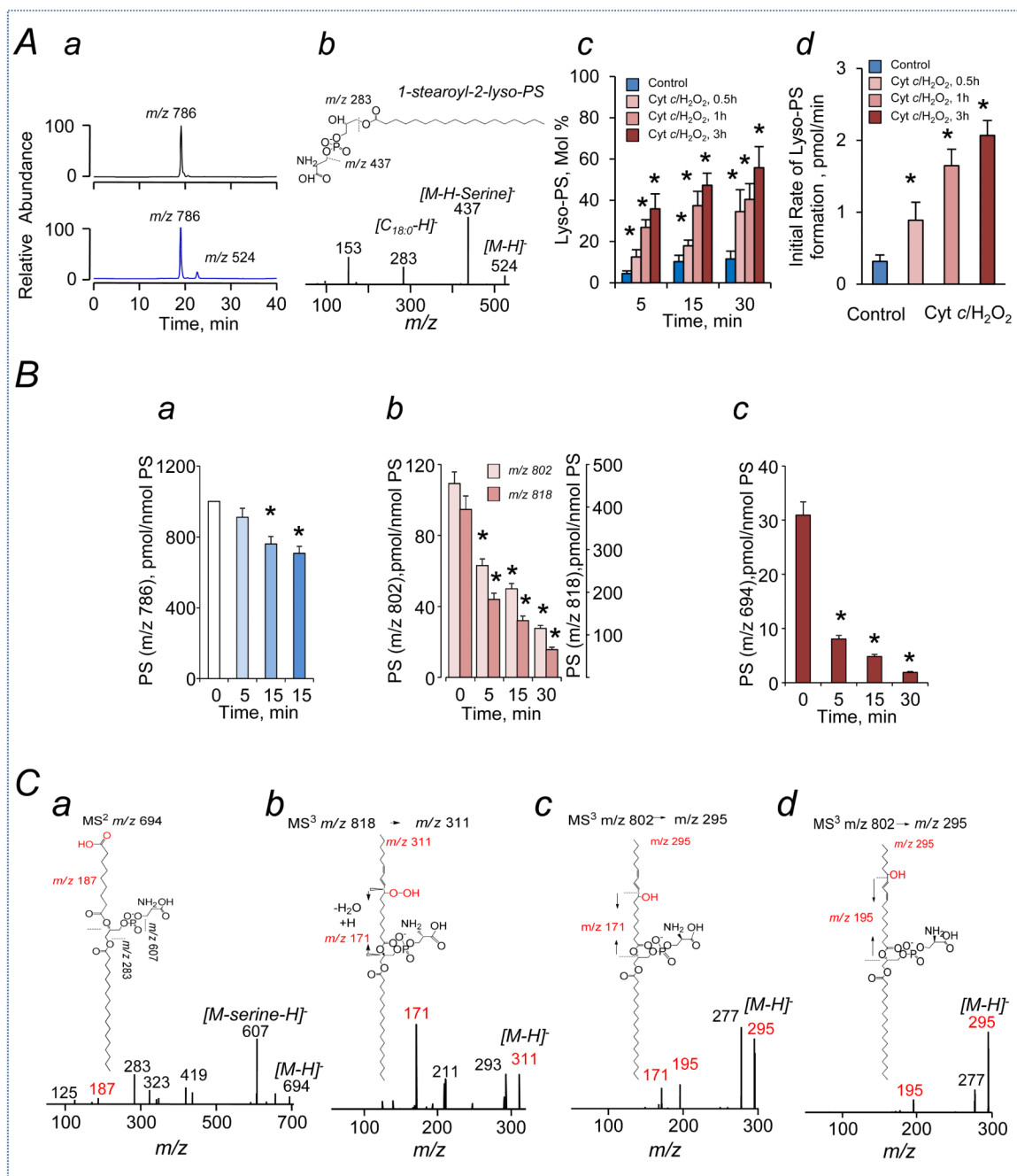
**Figure 1.**

LC-ESI-MS detection and structural characterization of SL-PS oxidation molecular species formed in cyt *c* driven reaction in the presence of  $H_2O_2$ .

**A.** Typical reconstructed LC-ESI-MS profiles of non-oxidized ( $m/z$  786) and oxidized ( $m/z$  818 and 850) SL-PS molecular species that contained 2 and 4 oxygens, respectively. Peak at  $m/z$  762 corresponded internal standard PS ( $C_{17:0}/C_{17:0}$ ).

**B.**  $MS^1$  spectra of SL-PS before (front panel) and after its oxidation during 30 min induced by cyt *c*/ $H_2O_2$  (back panel). Molecular ions corresponding to SL-PS containing 1-4 oxygens are detected on MS spectrum.

**C.** Quantitative assessment of oxidized molecular species of SL-PS.

**Figure 2.**

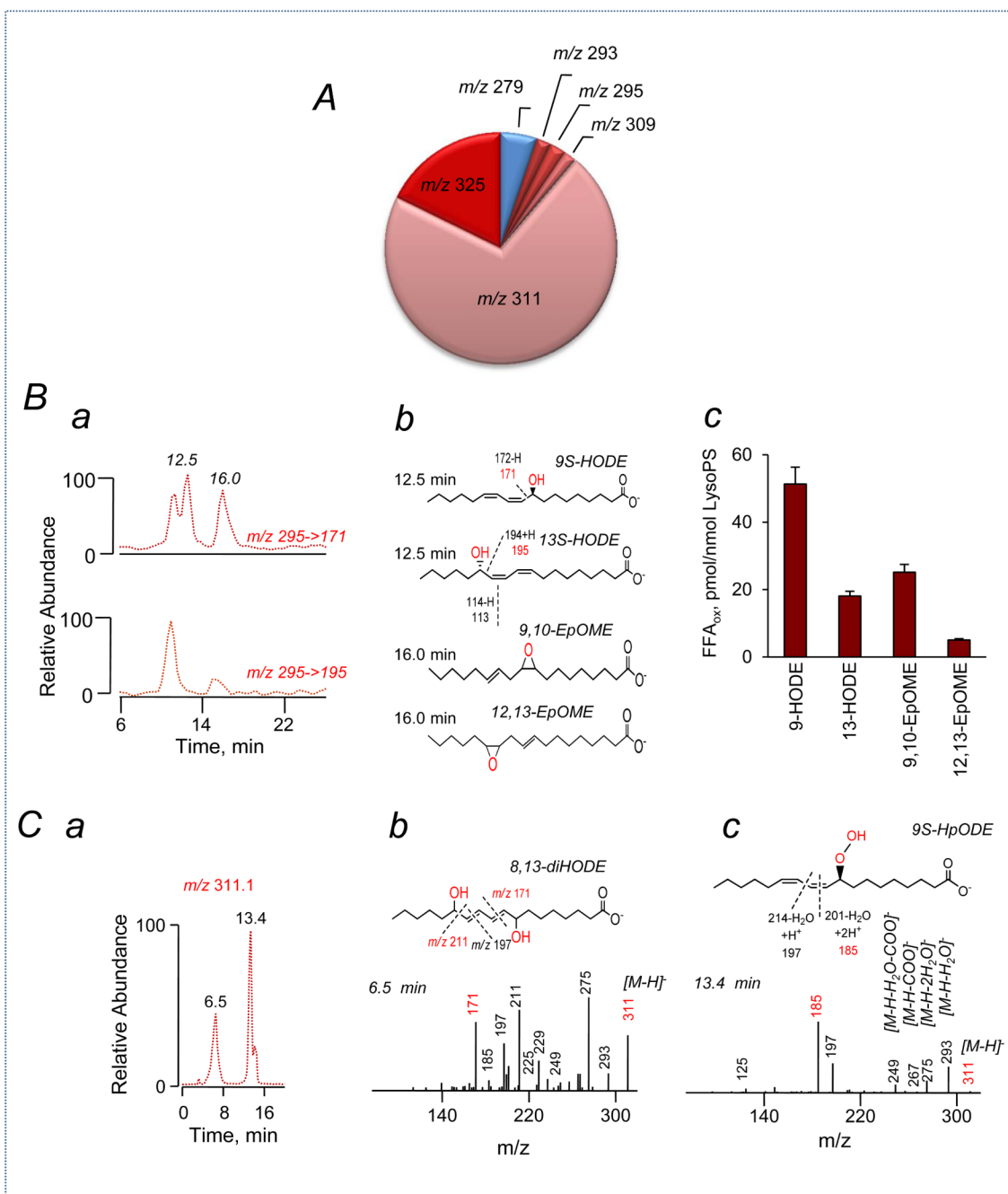
LC-ESI-MS detection and structural characterization of products formed after Lp-PLA<sub>2</sub>-catalyzed hydrolysis of oxidized SL-PS.

**A.** (a) Typical normal phase LC-ESI-MS profiles of SL-PS before and after hydrolysis by LpPLA<sub>2</sub>, (upper and lower panels, respectively). (b) MS<sup>2</sup> spectrum of lyso-PS molecular species formed after the hydrolysis and characteristic fragments of lyso-PS (m/z 524) (lower panel) with its chemical structure are shown (upper panel). (c) Quantitative assessment of 1-acyl-2-lyso-PS formed after hydrolysis of non-oxidized (control) and oxidized (by cyt *c*/H<sub>2</sub>O<sub>2</sub>, after 0.5; 1 and 3h) SL-PS at different time points. (d) Initial rate of non-oxidized and

oxidized SL-PS hydrolysis by LpPLA<sub>2</sub>. (Each value represents the mean + S.D. of at least three separate experiments).

**B.** Quantitative assessment of non-oxidized (**a**) and oxidized (by cyt c/H<sub>2</sub>O<sub>2</sub>, after 3h) individual SL-PS species (**b, c**) during hydrolysis by Lp-PLA<sub>2</sub>. Note that efficiency of Lp-PLA<sub>2</sub> in hydrolyzing SL-PSox species was proportional to the amount of oxygens present in the acyl chains. Oxidatively truncated species were preferable substrates for Lp-PLA<sub>2</sub>.

**C.** (**a**) Typical MS<sup>2</sup> spectrum of parent ion with m/z 694 corresponding to oxidatively fragmented ON PS molecular species. Insert: Chemical structure and MS<sup>2</sup> fragmentation patterns of molecular ion with m/z 694. (**b**) Typical MS<sup>3</sup> spectrum of daughter ion with m/z 311 formed during fragmentation of parent ion with m/z 818 corresponding to 9S-hydroperoxy-SL-PS molecular species. Insert: Chemical structure and MS<sup>3</sup> fragmentation patterns of molecular ion with m/z 818. (**c**) Typical MS<sup>3</sup> spectrum of daughter ion with m/z 295 formed during fragmentation of parent ion with m/z 802 corresponding to hydroxy-SL-PS molecular species. Insert: Chemical structure and MS<sup>3</sup> fragmentation patterns of molecular ion with m/z 802. (**d**) Typical MS<sup>3</sup> spectrum of daughter ion with m/z 295 formed during fragmentation of parent ion with m/z 802 after hydrolysis of hydroxy-SL-PS molecular species by Lp-PLA<sub>2</sub>. Insert: Chemical structure and MS<sup>3</sup> fragmentation patterns of molecular ion with m/z 802. In this series of experiment SL-PS was oxidized during 3h. Note: (**c, d**) Fragments with m/z 171 and 195 corresponding to 9- and 13-oxygenated carboxylate anions of linoleic acid, respectively, were detected in MS<sup>3</sup> spectrum of SL-PSox (m/z 802>295). Hydrolysis of SL-PSox by Lp-PLA<sub>2</sub> result in elimination of fragment with m/z 171 from MS<sup>3</sup> spectrum, only fragment with m/z 195 was observed in the in MS<sup>3</sup> spectrum obtained from parent ion with m/z 802. Thus hydrolysis of SL-PSox by Lp-PLA<sub>2</sub> results in selective release of oxidized linoleic corresponding to C9-hydroxy molecular species linoleic acid.

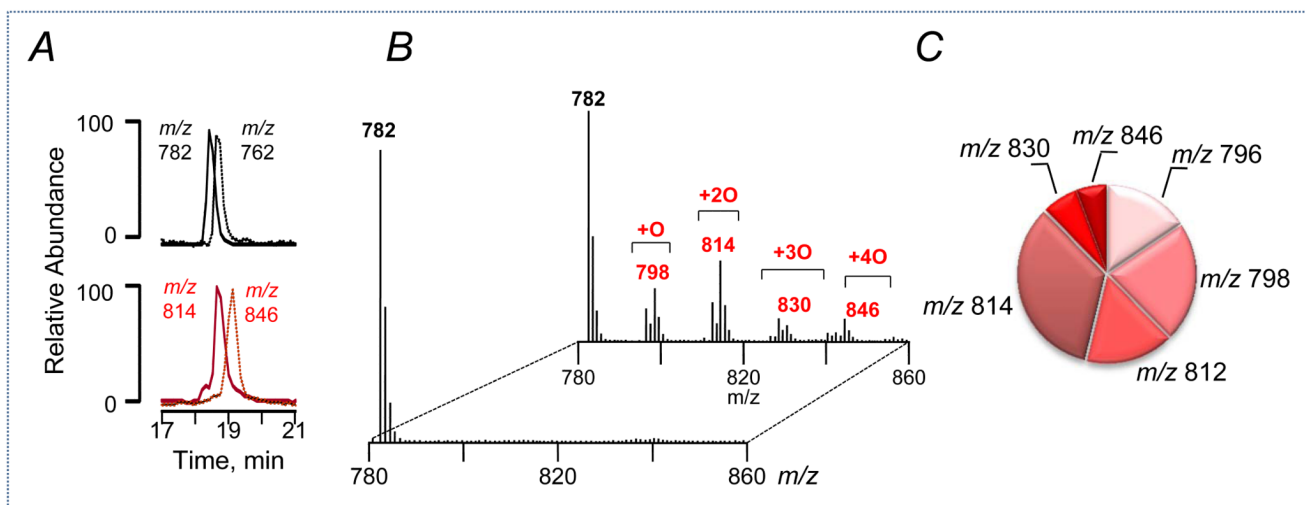
**Figure 3.**

Structural characterization of FFA released from SL-PS after its hydrolysis by Lp-PLA<sub>2</sub>.  
**A.** Quantitative assessment of fatty acids released from SL-PS after its hydrolysis by Lp-PLA<sub>2</sub>.

**B. (a)** Typical reverse phase LC-ESI-MS reconstructed profiles of the SRM for  $m/z$  295 with appropriate mass transitions as noted are shown on the upper panel (295>171) and lower panel (295>195) **(b)**. FFA chemical structures with possible position of oxygenated group on side chain are shown. Peaks with retention time 11-12 min are corresponded to 9S-HODE ( $m/z$  171) and 13S-HODE ( $m/z$  195), respectively. Peaks with retention time 16 min are corresponded to 9,10-epoxy- C<sub>18:2</sub> ( $m/z$  171) and 12,13-epoxy-C<sub>18:2</sub> ( $m/z$  195),

respectively. (c). Quantitative assessment of hydroxy- and epoxy-linoleic acids released from SL-PS after its hydrolysis by PLA<sub>2</sub>.

C. (a) Typical reverse phase LC-ESI-MS reconstructed profiles of free oxidized linoleic acid at m/z 311 formed after hydrolysis of SL-PSox by Lp-PLA<sub>2</sub>. (b, c, **lower panels**) MS<sup>2</sup> spectra (C18:2-OO, retention times 6.5 and 13.4 min, respectively) at m/z 311 formed after hydrolysis of SL-PSox by Lp-PLA<sub>2</sub> and chemical structures with possible position of oxygenated group on side chain are shown (**upper panels**).



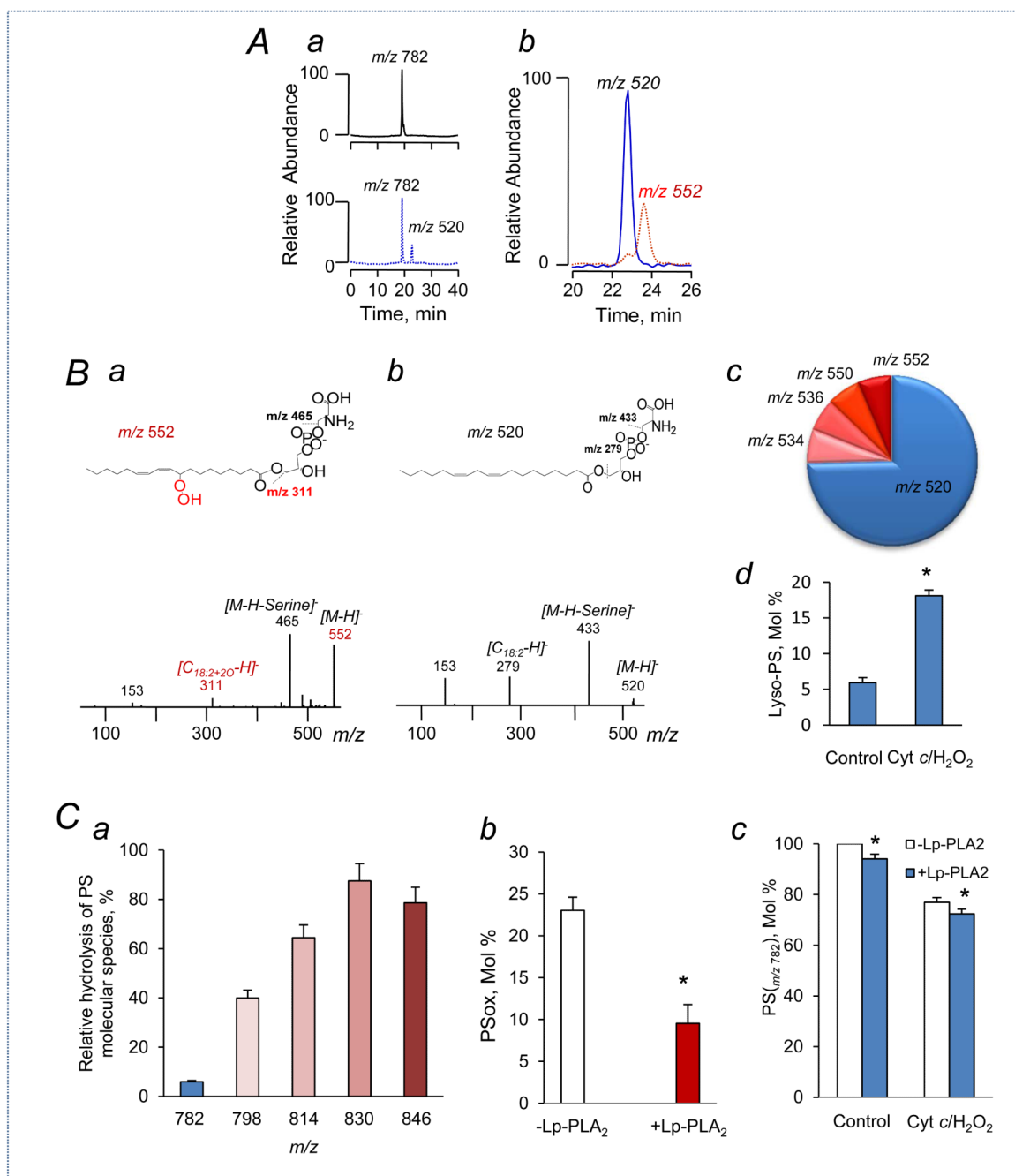
**Figure 4.**

LC-ESI-MS detection and structural characterization of LL-PS oxidation molecular species formed in *cyt c* driven reaction in the presence of  $H_2O_2$ .

**A.** Typical reconstructed LC/ESI-MS profiles of non-oxidized ( $m/z$  782) and oxidized ( $m/z$  814 and 846) LL-PS molecular species that contained 2 and 4 oxygens, respectively. (**b**) Peak at  $m/z$  762 corresponded internal standard PS ( $C_{17:0}/C_{17:0}$ ).

**B.**  $MS^1$  spectra of LL-PS before (front panel) and after its oxidation during 30 min induced by *cyt c*/ $H_2O_2$  (back panel). Molecular ions corresponding to SL-PS containing 1-4 oxygens are detected on MS spectrum.

**C.** Quantitative assessment of oxidized molecular species of LL-PS.

**Figure 5.**

LC-ESI-MS detection and structural characterization of lyso-PS formed from LL-PS after hydrolysis by Lp-PLA<sub>2</sub>.

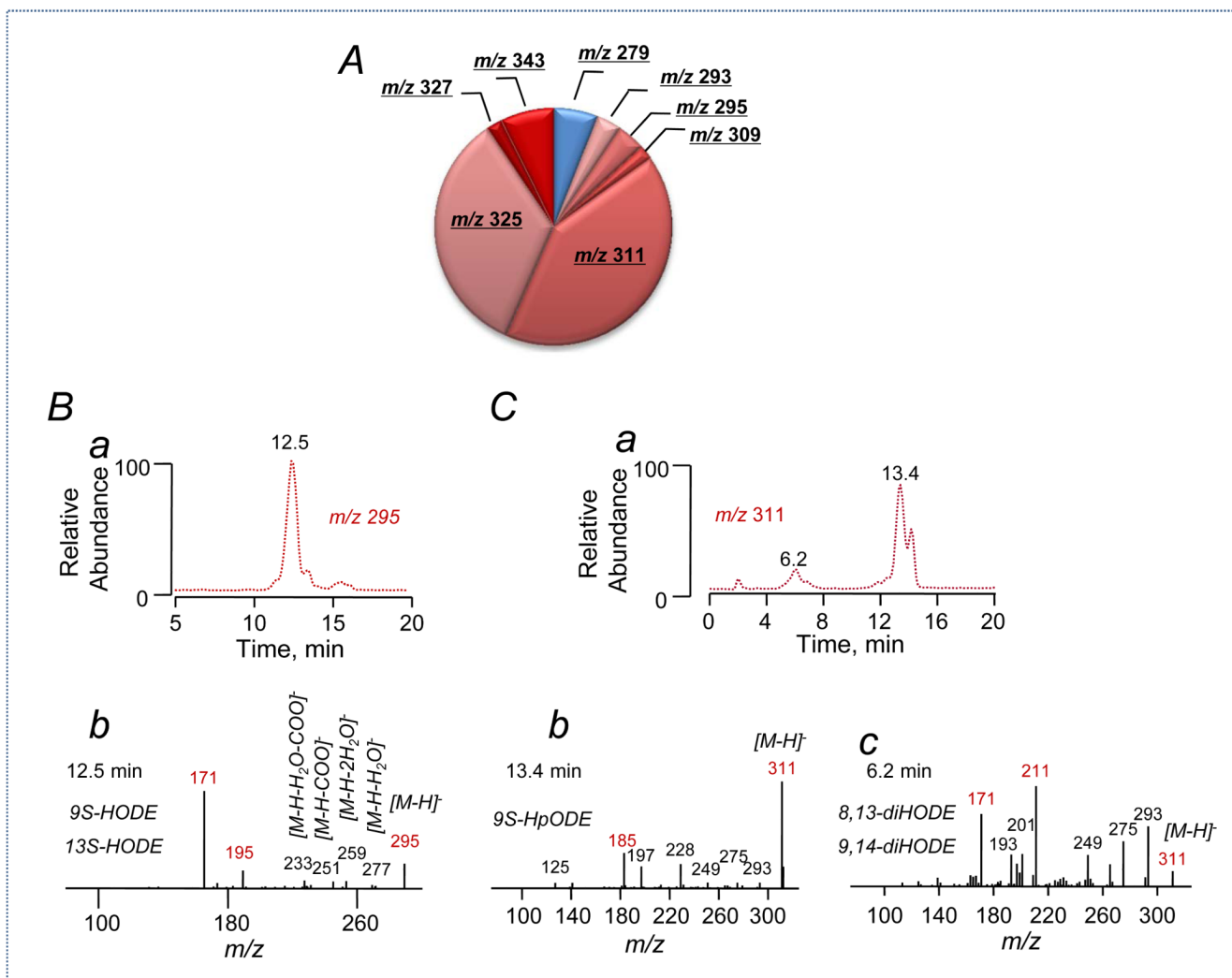
**A.** Typical normal phase LC-ESI-MS profiles of LL-PS (**a**, upper left panel) and 1-acyl-2-lyso-PS (**a**, lower left panel, and **b**) formed after hydrolysis of LL-PS and LL-PSox by Lp-PLA<sub>2</sub>.

**B.** MS<sup>2</sup> spectra of lyso-PS molecular species formed after its hydrolysis. Characteristic fragments of lyso-PS ( $m/z$  552 (**a**, lower panel) and  $m/z$  520 (**b**, lower panel)) and their chemical structure are shown (**a**, **b** upper panels). (**c**) Quantitative assessment of lyso-PS formed after hydrolysis of LL-PSox by Lp-PLA<sub>2</sub>. (**d**) Quantitative assessment of 1-acyl-2-

lyso-PS formed after hydrolysis of non-oxidized (control) and oxidized (cyt *c*/H<sub>2</sub>O<sub>2</sub>, 30 min) LL-PS. (Each value represents the mean ± S.D. of at least three separate experiments).

**C. (a)** Preferable hydrolysis of oxidized LL-PSox individual molecular species by Lp-PLA<sub>2</sub>. Relative hydrolysis efficiency of individual SL-PS molecular species by Lp-PLA<sub>2</sub> is shown. **(b)** Quantitative assessment of oxidized LL-PS species during hydrolysis by Lp-PLA<sub>2</sub>. **(c)** Quantitative assessment of non-oxidized LL-PS (*m/z* 782) before and after its incubation with cyt *c*/H<sub>2</sub>O<sub>2</sub> during hydrolysis by Lp-PLA<sub>2</sub>.



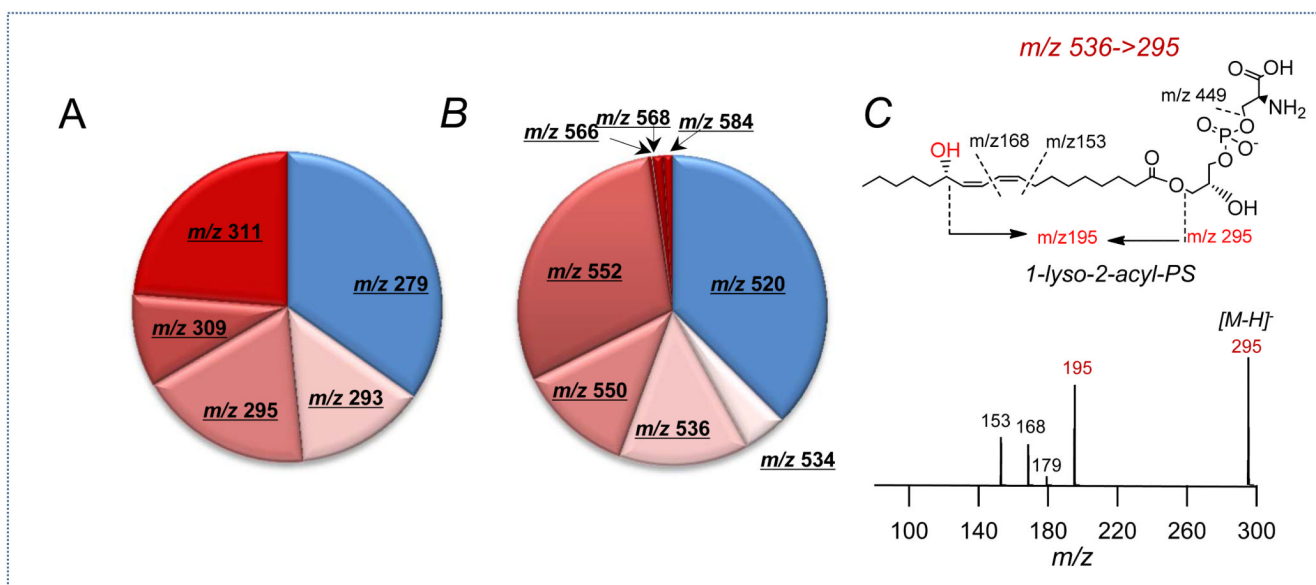


**Figure 6.** Structural characterization of free fatty acids released from LL-PS after their hydrolysis by Lp-PLA<sub>2</sub>.

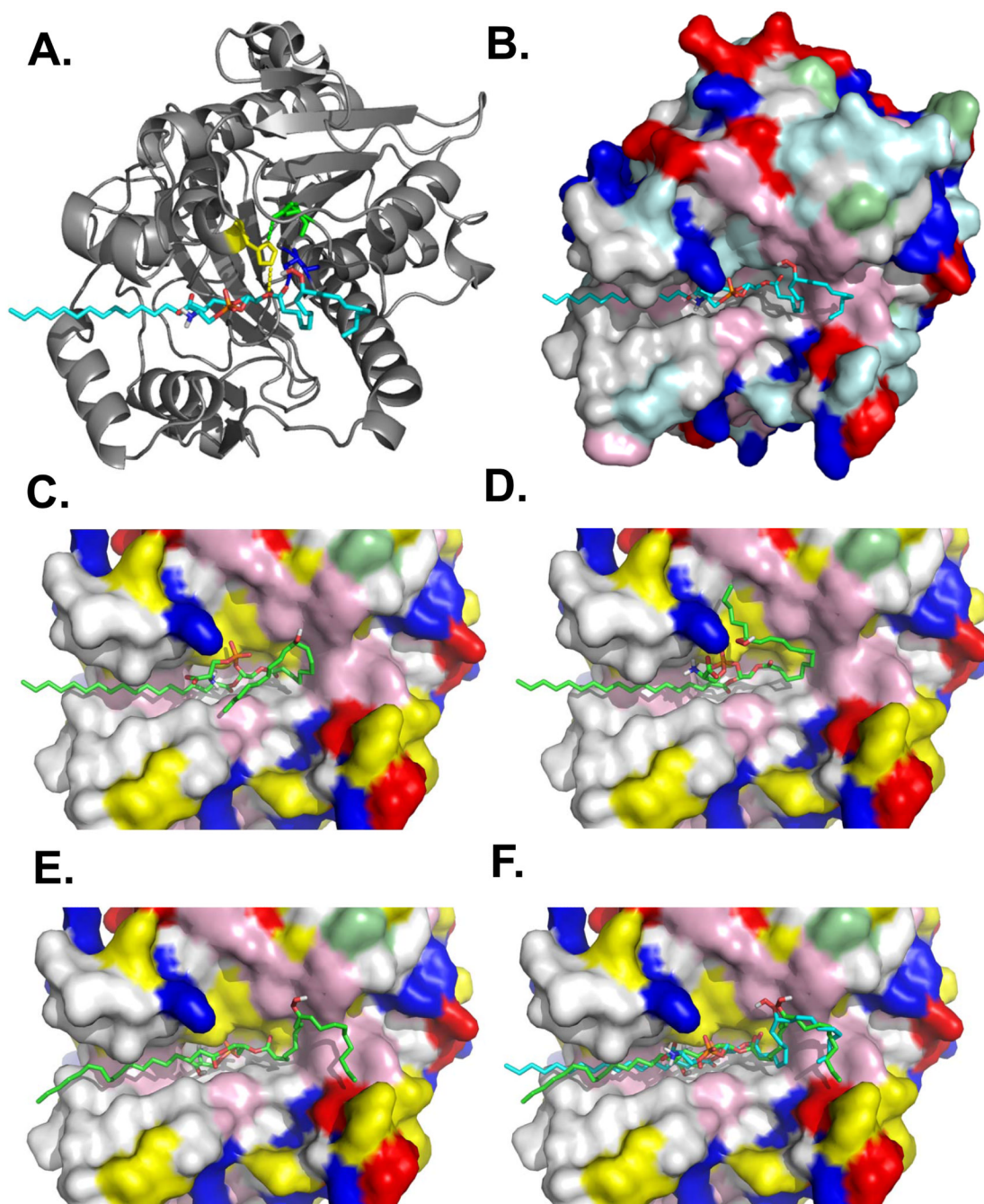
**A.** Quantitative assessment of fatty acids released from LL-PS after its hydrolysis by Lp-PLA<sub>2</sub>.

**B.** Typical reverse phase LC-ESI-MS reconstructed profile (*a*) and MS<sup>2</sup> spectrum (*b*) of oxygenated linoleic acid (*m/z* 295) released after hydrolysis of LL-PSox by Lp-PLA<sub>2</sub>.

**C.** Typical reverse phase LC-ESI-MS reconstructed profiles (*a*) and MS<sup>2</sup> spectra (*b*, *c*) of free oxidized linoleic acid (C<sub>18:2</sub>-OO, retention times 6.5 and 13.4 min, respectively) at *m/z* 311 formed after hydrolysis of LL-PSox by Lp-PLA<sub>2</sub>.



**Figure 7.**  
Structural characterization of free fatty acids released from LL-PS after their hydrolysis by PLA<sub>1</sub>.  
**A.** Quantitative assessment of FFA released from LL-PS after its hydrolysis by PLA<sub>1</sub>.  
**B.** Quantitative assessment of lyso-PS released from LL-PS after its hydrolysis by PLA<sub>1</sub>.  
**C.** MS<sup>3</sup> spectrum of oxidized lyso-PS molecular species with  $m/z$  536 (lower panel) and its possible chemical structure (upper panel) are shown.



**Figure 8.** Molecular models of oxidized SL-PS and LL-PS bound to the crystal structure of Lp-PLA<sub>2</sub>. (A). Cartoon representation of Lp-PLA<sub>2</sub> in complex with a hydroperoxy group at C<sub>9</sub> position of SL-PS. The residues corresponding to the catalytic triad, Ser<sub>273</sub>, Asp<sub>296</sub>, and His<sub>351</sub> are colored in blue, green and yellow, respectively and rendered as sticks. The close proximity of the Ser<sub>273</sub> side chain 'O' to *sn*-2 carbonyl 'O' and His<sub>351</sub> 'N' atom to the *sn*-2 ester 'O' atom is highlighted using blue and yellow dashes, respectively. Surface representation of Lp-PLA<sub>2</sub> with the predicted binding poses for hydroperoxy at C<sub>9</sub>, hydroxyl at C<sub>9</sub> position, and hydroperoxy at C<sub>13</sub> position of SL-PS is shown in (B), (C) and (D), respectively. The predicted binding interface of the (E) hydroperoxy group at C<sub>9</sub> position of LLPS and (F) an

overlay of hydroperoxy group at C<sub>9</sub> position for both SL-PS (with carbons colored in cyan) and LL-PS species (with carbons colored in green). The surface is colored based on residue type in **B-F**. The residues corresponding to polar-, hydrophobic-, aromatic-, positively charged-, and negatively charged residues are colored in the order yellow, white, magenta, blue and red. The SL-PSox and LL-PSox are rendered as sticks in all cases. The Images were generated using Pymol software.<sup>(68)</sup>

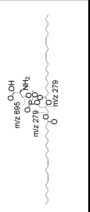

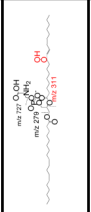
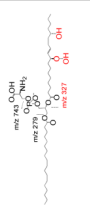
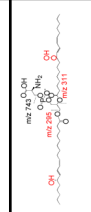
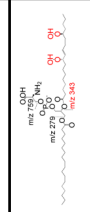
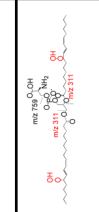
Table 1

Structural characterization of non-oxidized and oxidized SL-PS molecular species.

Parent ion, [M-H] <sup>-</sup>	[M-H-serine] <sup>-</sup>	[M-serine-R <sup>1</sup> CH <sub>2</sub> COO] <sup>-</sup>	[M-serine-R <sup>2</sup> CH <sub>2</sub> COO] <sup>-</sup>	[FA-H] <sup>-</sup> <i>sn</i> -1	[FA-H] <sup>-</sup> <i>sn</i> -2	Possible structure
786	699	415	419	283	279	
802	715	431	419	283	295	
818	731	447	419	283	311	
834	747	463	419	283	327	
850	763	479	419	283	343	

Note: SL-PS was analyzed by LC-ESI-MS using PQD mode. Chemical structure of five SL-PS regio-isomers and their characteristic fragments indicated positions of the hydroxy- or hydroperoxy- groups on the side chain are shown. Structural ESI-MS analysis of non-hydrolyzed SL-PS in negative mode revealed de-protonated ions [M-H]<sup>-</sup> with *m/z* 786. The peak with *m/z* 699 is formed during fragmentation of PS (*m/z* 786) due to the loss of the serine group (786-87). Molecular ions corresponding to stearic and linoleic acids with *m/z* 283 and 279, respectively, were detected on MS spectrum as well. Fragments of [M-serine-RCH<sub>2</sub>COOH]<sup>-</sup> corresponding to *m/z* 415, 419 were identified as daughter ions without fatty acid from *sn*-1 and *sn*-2 positions, respectively. MS<sup>2</sup> fragmentation of oxygenated SL-PS revealed the appearance of peaks at *m/z* 715, 731 747 and 763 formed due to loss of the serine group (802-87, 818-87 and 834-87). Ions with *m/z* 419 formed after the loss of oxidized linoleic acid a detected in the MS spectra. Appearance of carboxylate anions at *m/z* 295, 311 and 327 indicated that oxidized acyl chains from *sn*-2 position of the glycerol backbone were also detected on MS<sup>2</sup> spectra. Detailed MS<sup>2</sup> analysis demonstrated that the PS [M-H]<sup>-</sup> ions at *m/z* 802, 818, 834 and 850 corresponded to the PS species (C18:0/C18:2+O), (C18:0/C18:2+2O), (C18:0/C18:2+3O) and (C18:0/C18:2+4O), respectively.

**Table 2**  
Structural characterization of non-oxidized and oxidized LL-PS molecular species.

Parent ion, [M-H] <sup>-</sup>	[M-H-serine] <sup>-</sup>	[M-serine-R <sup>1</sup> CH <sub>2</sub> COO] <sup>-</sup>	[M-serine-R <sup>2</sup> CH <sub>2</sub> COO] <sup>-</sup>	[FA-H] <sup>-</sup> <i>sn</i> -1	[FA-H] <sup>-</sup> <i>sn</i> -2	Possible structure
782	695	415	415	279	279	
798	711	431	415	279	295	
814	727	447	415	279	311	
830	743	463	415	279	327	
830	743	447	431	295	311	
846	759	479	415	279	343	
846	759	447	447	311	311	

Note: Structural ESI-MS analysis of LL-PS in negative mode revealed de-protonated ions [M-H]<sup>-</sup> with *m/z* 782. The peak with *m/z* 695 formed after fragmentation of PS molecular ion with *m/z* 782 was due to a loss of the serine group (782-87). In addition, fragmentation yielded two ions at *m/z* 415 via losses of C<sub>18:2</sub> from molecular ion with *m/z* 695. Molecular ion with *m/z* 279 corresponding to carboxylate anion of linoleic acid localized either at *sn*-1 or *sn*-2 position of glycerol backbone was also detected on MS spectrum. MS<sup>2</sup> fragmentation of molecular ions corresponding to oxidized molecular species of LL-PS with *m/z* 798, 814, 830 and 846 revealed appearance of peaks at *m/z* 711, 727, 743 and 759 formed due to the loss of the serine group (798-87, 814-87, 830-87 and 846-87, respectively). Molecular ions with *m/z* 295, 311, 327 and 343 corresponding to oxygenated linoleic acid with 1-4 oxygen were also observed on MS spectra. Chemical structure of seven LL-PS regioisomers and their characteristic fragments utilized to characterize position of the hydroxy- or hydroperoxy- groups on the side chain are shown.

Table 3

Parameters obtained from molecular docking of non-oxidized and oxidized SL-PS/LL-PS species to the Lp-PLA2 structure using Autodock Vina (see Methods). The reported score corresponds to the lowest binding energy in each case.

<i>sr-2</i> Species	PS (C <sub>18:0</sub> /C <sub>18:2</sub> )		PS (C <sub>18:2</sub> /C <sub>18:2</sub> )	
	Predicted Binding Energy (number of conformations)	S <sub>273</sub> (Å)	H <sub>451</sub> (Å)	Predicted Binding Energy (number of conformations)
Non-oxidized	-6.5 (1)	4.42	6.41	-6.2 (1)
*C <sub>9</sub> -O	-7.3 (4)	2.75	3.33	-8.3 (3)
*C <sub>9</sub> -OOH	-7.3 (6)	2.83	3.28	-7.3 (5)
-9OH	-7.5 (3)	2.89	3.46	-7.5 (4)
-9OOH	-7.4 (5)	2.89	3.13	-7.9 (6)
-9OH-14OH	-7.8 (5)	2.81	3.6	-7.3 (5)
-9OOH-14OOH	-6.8 (3)	3.17	3.09	-7.2 (5)
-9OH-(12,13)O	-6.8 (1)	2.98	4.28	-6.7 (1)
-13OH	[ <i>a</i> ]	- <i>a</i> )	- <i>a</i> )	- <i>a</i> )
-13OOH	-7.4 (1)	5.23	3.9	-6.2 (1)

Note: The predicted binding energy in Kcal/mol along with the total number of conformers bound in close proximity to the active site is provided in each case i.e., for the SL-PS/LL-PS and various SL-PSox/LL-PSox species. Furthermore, the distances between Ser273 side chain 'O' to *sr-2* carbonyl 'O' and His251 'N' atom to the *sr-2* ester 'O' atom are listed for the conformation with where the distance was shortest.

\* denotes truncated species.

*a*) None of the predicted binding poses for 13-OH were in close proximity to the active catalytic site of PLA<sub>2</sub>. For this reason, no results are reported for 13-OH, based on our selection criteria as detailed in methods section.

**Table 4**

Amino acids in proximity to OH and OOH groups on oxidized lipids. Bound ligand conformations predicted by Autodock Vina are numbered according to their rank 1-9 and their identity is given in brackets behind the contact residue. Only PS (C<sub>18:0</sub>/C<sub>18:2</sub>) were evaluated.

<i>sn</i> -2 Species	Contact residue(s) [Conformation(s)]	
*C <sub>9</sub> -O	Phosphate of PS [2,4], Phe322 [2,4], Arg218 [5], Gln211 [6], Glu214 [6]	
*C <sub>9</sub> -OOH	Phosphate of PS [1,6], Phe322 [2], Arg218 [3], Glu214 [3], Phe110 [4], Tyr324 [5], Trp298 [5]	
-9OH	Phosphate of PS [1], Tyr324 [2], none [3]	
-9OOH	Phosphate of PS [1,2,3], Tyr324 [1,2,3], Phe322 [1,2,3], Glu214 [4], Arg218 [4], none [6]	
-9OH-14OH	-9OH	-14OH
	Amine of PS [1], Phe322 [1], Tyr 321 [2], Glu214 [3], Trp298 [3], Tyr324 [4,6], Trp298 [6]	Phe110 [1], Leu111 [1], Amine of PS [2], none [3,4], Glu214 [6]
-9OOH-14OOH	-9OOH	-14OOH
	Phe322 [1], none [2], Tyr324 [3]	Leu111 [1], none [2,3]